In: Building Materials: Properties, Performance and Applications ISBN: 978-1-60741-082-9
Editors: Donald N. Cornejo and Jason L. Haro

Chapter 9

AGRICULTURAL WASTES AS BUILDING MATERIALS: PROPERTIES, PERFORMANCE AND APPLICATIONS

José A. Rabi*[*], *Sérgio F. Santos*[†], *Gustavo H. D. Tonoli*[≠] and *Holmer Savastano Jr.*[‡]
Faculty of Animal Science & Food Engineering (FZEA), University of São Paulo (USP)
Avenida Duque de Caxias Norte, 225, 13635-900, Pirassununga, SP, Brazil

ABSTRACT

While recycling of low added-value residual materials constitutes a present day challenge in many engineering branches, attention has been given to cost-effective building materials with similar constructive features as those presented by materials traditionally employed in civil engineering. Bearing in mind their properties and performance, this chapter addresses prospective applications of some elected agroindustrial residues or by-products as non-conventional building materials as means to reduce dwelling costs.

Such is the case concerning blast furnace slag (BFS), a glassy granulated material regarded as a by-product from pig-iron manufacturing. Besides some form of activation, BFS requires grinding to fineness similar to commercial ordinary Portland cement (OPC) in order to be utilized as hydraulic binder. BFS hydration occurs very slowly at ambient temperatures while chemical or thermal activation (singly or in tandem) is required to promote acceptable dissolution rates. Fibrous wastes originated from sisal and banana agroindustry as well as from eucalyptus cellulose pulp mills have been evaluated as raw materials for reinforcement of alternative cementitious matrices, based on ground BFS.

Production and appropriation of cellulose pulps from collected residues can considerably increase the reinforcement capacity by means of vegetable fibers. Composites are prepared in a slurry dewatering process followed by pressing and cure under saturated-air condition. Exposition of such components to external weathering leads to a significant long-term decay of mechanical properties while micro-structural

* jrabi@usp.br
† sfsantos1@usp.br
≠ gustavotonoli@usp.br
‡ holmersj@usp.br

analysis has identified degradation mechanisms of fibers as well as their mineralization. Nevertheless, these materials can be used indoors and their physical and mechanical properties are discussed aiming at achieving panel products suitable for housing construction whereas results obtained thus far have pointed to their potential as cost-effective building materials.

Phosphogypsum rejected from phosphate fertilizer industries is another by-product with little economic value. Phosphogypsum may replace ordinary gypsum provided that radiological concerns about its handling are properly overcome as it exhales radon-222, a gaseous radionuclide whose indoor concentration should be limited and monitored. Some phosphogypsum properties of interest (e.g., bulk density, consistency, setting time, free and crystallization water content, and modulus of rupture) have indicated its large-scale exploitation as surrogate building material.

INTRODUCTION

Developing countries usually face grave housing deficits and the following hurdles against dwelling construction have been typically pointed out: high interest rates, elevated social taxes, high informal labor indexes, and bureaucracy. Lack of loan is an additional problem[1] as banks may not be interested on funding or because governmental programs are scarce. As a result, a considerable percentage of the population in developing countries still lives at sub-dwelling units. In 2006, estimates suggested that around 7.9 million dwellings were needed in Brazil, most of them (83.3%) located in urban areas, particularly in the so-called Metropolitan Regions[2] surrounding Brazilian state capitals (2.2 million dwellings) [1]. Metropolitan Regions around São Paulo and Rio de Janeiro cities present the greatest housing deficits, adding together to almost 1.2 million dwellings [1].

Aiming at lowering costs, scientific attention has been given to non-conventional building materials with similar features as those presented by construction materials traditionally used in civil engineering. Quest for such surrogate materials can be two-fold interesting as (*i*) it may help to reduce dwelling deficits (particularly in developing countries) inasmuch as cheaper houses become economically feasible and (*ii*) it can be environmentally friendly as low-value wastes can be recycled or exploited. Accordingly, this chapter is particularly interested in agroindustrial residues or by-products as prospective non-conventional construction materials.

VEGETABLE FIBERS AS NON-CONVENTIONAL BUILDING MATERIAL

Vegetable fibers are widely available in most developing countries. They are suitable reinforcement materials for brittle matrix even though they present relatively poor durability performance. Accounting for the mechanical properties of the fibers as well as their broad variation range, one may develop building materials with suitable properties by means of the adequate mix design [2], [3].

1 This is particularly true during economic and financial crisis such as the worldwide crisis started in 2008.

2 Metropolitan Regions of major interest in Brazil refer to the following capitals (corresponding state in brackets): Belém (Pará), Fortaleza (Ceará), Recife (Pernambuco), Salvador (Bahia), Belo Horizonte (Minas Gerias), São Paulo (São Paulo), Rio de Janeiro (Rio de Janeiro), Curitiba (Paraná), and Porto Alegre (Rio Grande do Sul).

The purpose of the fiber reinforcement is to improve mechanical properties of a given building material, which would be otherwise unsuitable for practical applications [4]. A major advantage concerning fiber reinforcement of a brittle material (e.g., cement paste, mortar, or concrete) is the composite behavior after cracking. Post-cracking toughness produced by fibers in the material may allow large-scale construction use of such composites [4].

There are two approaches for the development of new composites in fiber-cement [5]. The first one is based on the production of thin sheets and other non-asbestos components. The later components are similar to asbestos-cement ones and they are produced by well-known industrial-scale processes such as Hatschek and Magnani methods commercially used with high acceptance for building purposes [6]. The second approach consists of producing composites for different types of building components like load-bearing hollowed wall, roofing tiles, and ceiling plates, which are not similar to components commercially produced with asbestos-cement.

Estimated as several million of tons per year [7], consumption of fiber-reinforced cement building components is rapidly increasing, especially in developed countries. This is because such type of material allows one to produce lightweight building components with good mechanical performance (mainly regarding impact energy absorption) and suitable thermal-acoustic insulation, while being economically attractive [4]. Fibers naturally occur in tropical and equatorial countries, where they have been essentially targeted to cordage, textile, and papermaking sectors. Their heterogeneity and perishing allied to restricted market for their use have lead to intense generation of residues with high pollution potential. For example, each ton of commercially used sisal fibers yields three tons of residual fibers, whose dumping has originated environmental hazards [8].

Table 1. Physical or mechanical properties of some fibers.

Fiber	Property of interest				
	Density (g/cm^3)	Tensile strength (MPa) [e]	Modulus of elasticity (GPa)	Elongation at failure (%)	Water absorption (%)
Jute (*Corchorus capsularis*) [a]	1.36	400 - 500	17.4	1.1	250
Coir (*Cocos nucifera*) [b]	1.17	95 – 118	2.8 [d]	15 - 51	93.8
Sisal (*Agave sisalana*) [b]	1.27	458	15.2	4	239
Banana (*Musa cavendishii*) [a]	1.30	110 - 130	---	1.8 - 3.5	400
Bamboo (*Bambusa vulgaris*) [b]	1.16	575	28.8	3.2	145
E-glass [c]	2.50	2500	74	2 - 5	---
Polypropylene [c]	0.91	350 - 500	5 - 8	8 - 20	---

[a] [11], [b] [5], [c] [12], [d] [13]; [e] tensile strength strongly depends on the type of the fiber, being a bundle or a single filament.

As reported in Coutts [9], vegetable fibers contain cellulose (which is a natural polymer) as the main reinforcement material. The chains of cellulose form microfibrils, which are held together by hemicellulose and lignin in order to form fibrils. The later are then assembled in various layers to build up the fiber structure. Fibers or cells are cemented together in the plant by lignin, which can be dissolved by the cement matrix alkalinity [10]. The usual

denomination for fibers is indeed a reference to strands with significant consequences on durability studies.

Banana fibers cut from the plant pseudo-stem and sisal by-products from cordage industries are examples of widely available fibers. Eighteen types of potential fibers have been identified, including cellulose pulp recovered from newspaper, malva, coir, and sisal [5]. However, if costs and availability issues are accounted for, the number of suitable fiber types reduces drastically. Coir, sisal chopped strand fibers, and eucalyptus residual pulp have already been identified as fibrous waste materials suitable for cement reinforcement [8] and Table 1 presents some of their mechanical and physical properties of interest.

The present chapter is particularly interested in three different types of fibrous residues typically found in Brazil, namely:

- Sisal (*Agave sisalana*) field by-product: This material is readily available (e.g., 30,000 tons per year from a given producers' association) and it has presently no commercial value. Its use offers an interesting additional income for rural producers and simple manual cleaning via a rotary sieve provides a suitable starting-point material.
- Banana (*Musa cavendishii*) pseudo-stem fibers. This by-product has high potential availability from fruit production (e.g., 95,000 ton per year, based on Brazil's main producing area). This material has no market value and a simple low-cost fiber extraction process is required.
- *Eucalyptus grandis* waste pulp. Accumulating from several Kraft and bleaching stages, this resource has low commercial value (USD 15/ton) and is readily available (e.g., 17,000 ton per year from one pulp industry in Brazil's southeast region). Disadvantages of this material include short fiber length and high moisture content (about 60% of dry mass).

Although chopped fibrous residues can be directly introduced into the cement matrix for reinforcement, further chemical processing of these residual fibers has proved to improve the performance of the building products [14]. Pulped fibers are preferred for composites production using slurry vacuum de-watering technique, which is a laboratory-scale crude simulation of Hatschek process. During the de-watering stage, pulp forms a net that retains cement grains. Small fibers remain homogeneously distributed in two directions (2-D) into the matrix [15] and this fact suggests some advantages of using sisal pulp (individualized fibers) in relation to sisal strand fibers [14]. Reinforcement is distributed into the composite leading to the effective capacity of reinforcing and bridging cracks during bending tests. Cellulose pulps can be produced from residual crops (non-wood) fibers or wood species, reaction with alkaline liquors (e.g., sodium hydroxide, i.e., Kraft process), or organic solvents (e.g., ethanol).

Low performance of natural fiber reinforced composites (NFRC) has been associated to the use of chopped strand fibers as reinforcement for ordinary brittle cement matrices produced by conventional dough mixing methods [5]. This has been identified as the main reason for the low acceptance of these products by the industry. Consequently, in several developing countries asbestos-cement remains the major composite in use although health hazards have become a major concern [16]. In view of that, agricultural residual fibers

discussed in this chapter were further prepared in order to fit their use and to achieve improved performance in the composites.

PHOSPHOGYPSUM AS NON-CONVENTIONAL BUILDING MATERIAL

Another research line has pointed to the replacement of ordinary gypsum (calcium sulphate hemihydrate). Basically composed by calcium sulphate dihydrate ($CaSO_4 \cdot 2H_2O$), gypsite is the raw material for the production of ordinary gypsum through thermal dehydration. Gypsum has been mainly consumed as constructive boards (panels) and as wall covering (on minor extent) but its large-scale use in developing countries may become restricted or economically unfeasible due to transportation costs from production sites (mines) to potential consumption places (e.g., large cities), which is the scenario observed in Brazil.

According to the Brazilian National Department of Mineral Production (subordinated to the Ministry of Mining and Energy) [17], around 98% of Brazil's gypsite mines adding up to 1.3×10^9 tons are located in northern or north-eastern states, namely, Pará (30.3%), Bahia (42.7%), and Pernambuco (25.1%). Altogether in 2007, their corresponding gypsite production comprised 1.9×10^6 tons so that 89% (1.7×10^6 tons) was due to Pernambuco state alone, located more than 2,400 km away from either Rio de Janeiro or São Paulo Metropolitan Regions (both in Brazil's southeast region). Compared to the USA (world's largest gypsum consumer and producer), Brazilian consumption is very low, not only due to the aforesaid transportation costs and logistics associated to gypsite mines but also due to related energy costs and lack of necessary facilities.

Conversely, growing demands for phosphate fertilizers have yielded enormous amounts of phosphogypsum for years worldwide [18]. Despite being essentially $CaSO_4 \cdot 2H_2O$, such material has currently little economic value due to environmental issues notably regarding radon-222 (^{222}Rn) exhalation. Together with its decay products, ^{222}Rn is a radioactive noble gas responsible for most human natural exposure to radiation and assessment of its exhalation rate is crucial for radiological protection design [19].

Half-life of ^{222}Rn (= 3.824 days) is long enough to allow its transport through porous media or open air. If inhaled, its progeny is relatively short-lived allowing its eventual decay to ^{210}Pb (half-life = 22.3 years) before removal by physiological clearance mechanisms. Lung cancer risk related to dangerous exposure to the radiation released from ^{222}Rn and from its short-lived decay products was addressed in the 1950s among uranium miners while indoor-air ^{222}Rn concentration issues were claimed in the 1970s. Since then, scientific attention to ^{222}Rn exposure has increased [20]. Initial evidence had pointed to soil as a major natural source for high indoor concentrations [21] but building materials can also play an important role [22].

Phosphogypsum has been simply piled up nearby phosphate fertilizers industrial units [23], this way requiring considerable open-air space. For inactive phosphogypsum stacks in the US territory, US EPA (Environmental Protection Agency) has once restricted ^{222}Rn exhalation rates to 0.74 $Bq \cdot m^{-2} \cdot s^{-1}$ [24]. Even so, large-scale application of phosphogypsum is a motivating dilemma and research has been conducted to overcome difficulties related to the disposal and handling of this waste. Feasible solutions have suggested its exploitation as soil amendment in agriculture, mine recovery, road base, and embankment filling.

Of particular interest, encouraging (i.e., radioactively safe) evidence has already become available for phosphogypsum use as a non-conventional building material with similar features as ordinary gypsum [25]. Bearing in mind indoor air ^{222}Rn concentration, a major concern refers to the maximum amount of phosphogypsum (pure or blended to building materials) to be present in constructive elements such as pre-fabricated blocks or panels for cost-effective dwellings. Relying on protection procedures as air renewal and/or building openings (doors and windows), limits must be set so as to avoid hazardous radiological impacts, thus enabling occupants to be exposed to tolerable levels[3], i.e., without considerably increasing naturally occurring doses.

In line with its agroindustrial expansion, the Brazilian phosphogypsum scenario could not be different so that millions of tons have been similarly piled-up close to fertilizers plants [23]. These fertilizers plants are located in Brazil's southeast (basically in Minas Gerais and São Paulo states), hence close to the biggest Metropolitan Regions of the country. Aiming at cost-effective dwellings, such strategic coincidence might be convenient while motivating for prospective application of phosphogypsum as a surrogate building material.

Engineering precaution should then be exercised in terms of both constructive aspects and of protection against ionizing radiation whose level should be as low as those recognized by federal regulations or international standards. For instance, the International Commission on Radiological Protection (ICRP) has recommended 200 up to 600 $Bq \cdot m^{-3}$ for indoor-air ^{222}Rn concentrations at residences and workplaces [26]. In Brazil, the National Commission for Nuclear Energy (CNEN) is the organization responsible for setting upper limits for indoor-air 222Rn concentrations at these two aforesaid human environments.

VEGETABLE FIBER-CEMENT: COMPONENT, COMPOSITE, AND PERFORMANCE

A main drawback of using vegetable fibers is their durability in a cementitious matrix and the compatibility between both phases. Alkaline media weaken most natural fibers, especially the vegetable ones, which are actually strands of individual filaments liable to get separated from one another. The mineralization phenomenon proposed elsewhere [27], [28] can be associated to the long-term loss of the composite tenacity. The severe degradation of exposed composites can also be attributed to the interfacial damages due to continuous volume changes exhibited by the porous vegetable fibers inside the cement matrix [29].

Settled at the Construction and Thermal Comfort Laboratory (Faculty of Animal Science and Food Engineering – FZEA, University of São Paulo – USP, Brazil), the Research Group on Rural Construction has adopted two approaches to improve the durability of vegetable fibers. One is based on fibers protection by coating to avoid the water effect, mainly alkalinity. The other approach aims at reducing the free alkalis within the matrix by developing low alkaline binders based on industrial and/or agricultural by-products [30]. Similar reduced alkalinity effect can be reached by fast carbonation process as presented in

[3] Those more acquainted to human comfort may realize that, as opposing to thermal environment, a "radiological comfort zone" concept is not applicable here as the ideal lower level will be always zero rather than a minimum value (below which there would be discomfort). Accordingly, one may think of a "radiological stress zone" whose lower threshold would correspond to a maximum acceptable ^{222}Rn concentration.

[31], [32]. Studies and strategies to improve durability of vegetable fibers have been basically carried out on two types of building components, namely, roofing tiles and flat sheets for wall panels. Methodologies and results obtained for each type of component are presented and discussed in the following sections.

ROOFING TILES

Cement-based roofing tiles containing vegetable fibers or particles for rural constructions have been reported elsewhere [33], [34], [35]. Better results for fiber-cement materials were found using refined pulp and slurry dewatering process, followed by pressing [36]. The improved composites performance may justify the increase in energy consumption during these procedures. Such production is based on vacuum dewatering followed by pressing and it can be worthy for undulated tile fabrication in the near future by using of natural fibers or agricultural residues.

Improving Tiles Performance By Accelerated Carbonation

The present study was carried out as an attempt to produce durable fiber-cement roofing tiles (approximate dimensions: 500 mm long, 275 mm wide, 8 mm thick) by slurry dewatering technique and using sisal (*Agave sisalana*) Kraft pulp as reinforcement. Effects of accelerated carbonation on physical and mechanical performances of vegetable fiber-reinforced cementitious tiles were evaluated along with their consequent behaviors after ageing. Cement raw materials mixture was prepared with approximately 40% of solids (comprising 4.7% sisal pulp, 78.8% cement, and 16.5% ground carbonate material).

Initial cure was carried out in controlled environment (i.e., temperature: 25 ± 2ºC, relative humidity - RH: 70 ± 5%) so that roofing tiles remained in moulds protected with plastic bags for two days. Afterwards, roofing tiles were removed from moulds and immersed in water for further 26 days. After total curing period (28 days), tiles were submitted to both physical and mechanical tests. Remaining tiles series were intended to soak and dry-accelerated ageing tests as well as to accelerated carbonation so that roofing tiles were tested in saturated condition after immersion in water for at least 24 h. Accelerated carbonation of roofing tiles was carried out in a climatic chamber providing environment saturated with carbon dioxide (CO_2) and controlled temperature (20^oC) and humidity (75% RH). Roofing tiles were submitted to climatic chamber environment during one week until complete carbonation of samples. Carbonation degree was estimated via exposure to 2% phenolphthalein solution diluted in anhydrous ethanol as described in [4].

Figure 1 shows cross-sections of tiles after the application of phenolphthalein solution so that violet regions refer to non-carbonated areas. Tiles that were not fast carbonated underwent carbonation in peripheral regions only (tile 1 in Figure 1), which probably occurred during exposure inside the laboratory environment itself. Cross-section of tile 2 (Figure 1) was not violet colored, indicating that it was fully carbonated after being exposed to accelerated carbonation.

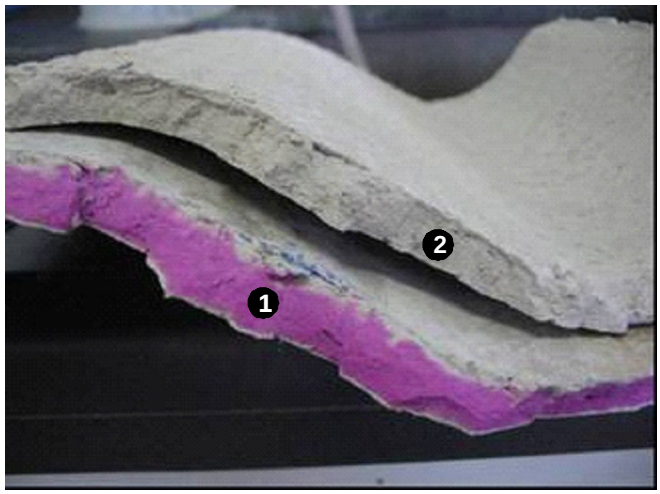

Figure 1. Cross-sections of tiles after the application of phenolphthalein solution: (tile 1) inner non-carbonated areas and (tile 2) areas exposed to fast carbonation.

Results for physical properties of undulated roofing tiles are presented in Table 2. Values for water absorption (WA), apparent void volume (AVV), and bulk density (BD) of roofing tiles for 28 days ageing (condition A) were similar to those found in [35] concerning the evaluation of roofing tiles produced with binder based on ground blast furnace slag (GBFS) reinforced with 3% by mass of sisal pulp and processed by vibration. Results in [35] for WA, AVV, and BD were 31.0%, 42.3%, and 1.35 g/cm^3, respectively.

Table 2. Average values and standard deviations for water absorption (WA), apparent void volume (AVV), and bulk density (BD) of roofing tiles under different conditions.

Condition	WA (%)	AVV (%)	BD (g/cm^3)
A (28 days)	32.8 ± 1.1	44.2 ± 0.7	1.35 ± 0.03
B (100 cycles)	33.3 ± 0.9	44.0 ± 0.9	1.32 ± 0.01
C (fast carbonation and 100 cycles)	23.3 ± 0.7	35.8 ± 1.8	1.56 ± 0.01

In general, ageing cycles contributed to mitigate leaching and to reduce porosity of roofing tiles. Accelerated carbonation followed by 100 cycles (condition C) was the treatment that most affected physical properties of roofing tiles. Porosity reduction provided by carbonation can be responsible for mechanical properties improvement while accelerated carbonation reduced tiles apparent void volume (AVV) by approximately 20%. Significant water absorption reduction and carbonated roofing tiles densification suggested the effective carbon dioxide absorption as well as the formation of new hydration products in the cement matrix. An estimated 15% reduction of cellulose fiber-cement porosity after its accelerated carbonation was also reported elsewhere [37].

Figure 2 presents typical load-deflection curves of roofing tiles. The maximum load (ML) supported by roofing tiles did not experience a significant reduction after ageing cycles. These results are considerably above the 425 N limit as recommended in [38] for 8 mm thick

tiles. Ageing (condition B) did not cause significant decrease in ML and toughness (TE) of roofing tiles in relation to non-aged tiles tested with 28 days (condition A). Moreover, ML and TE were superior to those found in preceding works with roofing tiles produced by vibration (Figure 2). ML and TE values around 550 N and 1.6 kN□mm, respectively, for roofing tiles reinforced with 2% (volume basis) of unrefined coir, sisal macro-fibers and eucalyptus waste pulp at 28 days of age were reported in [8].

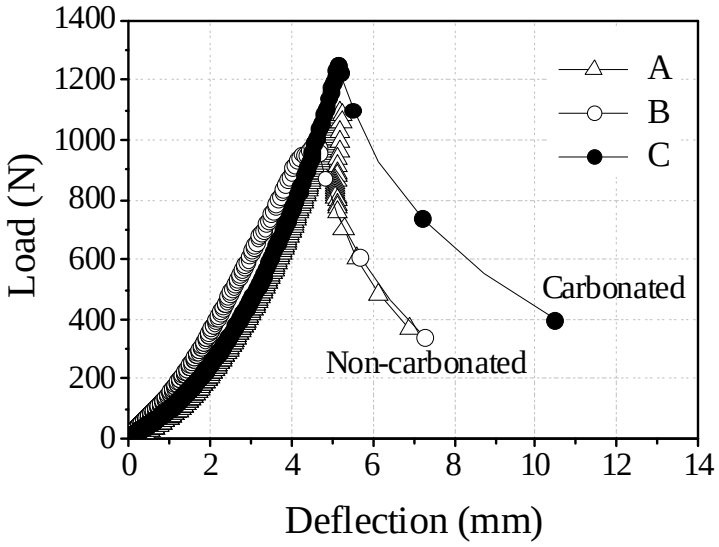

Figure 2. Load-deflection curves for tiles at different treatment conditions.

Pulp refinement and dispersion in the composite seem to contribute to homogeneous fibers distribution during roofing tiles molding, leading to better fibers anchorage in the matrix and thus improving the product strength. Among other variables, fibers net was more efficient at retaining cement particles during vacuum dewatering process, hence providing suitable packing during the pressing stage as well as more effective fiber-matrix bond. Figure 3 presents an image of the carbonated tile with refined sisal Kraft fiber, obtained via scanning electron microscope (SEM) and back-scattered electron (BSE) detector. The SEM-BSE image shows the advantage of refined fiber in generating a high contact area with the matrix.

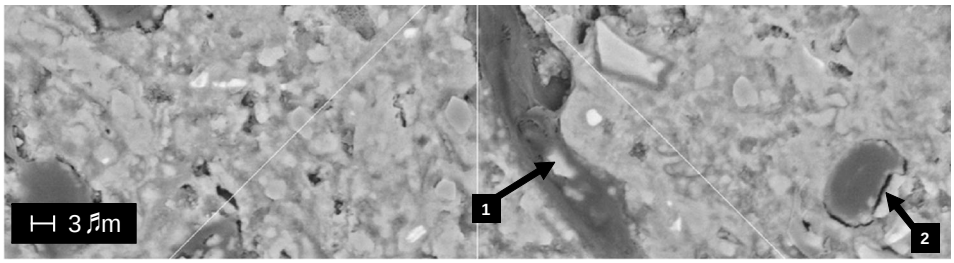

Figure 3. SEM-BSE image of fast carbonated and aged tile (condition C in Table 2).). Fibers are well adhered to matrix, suggesting good composite packaging. Arrows point to reprecipitated calcium hydroxide (1) inside fiber lumen and (2) around fiber surface.

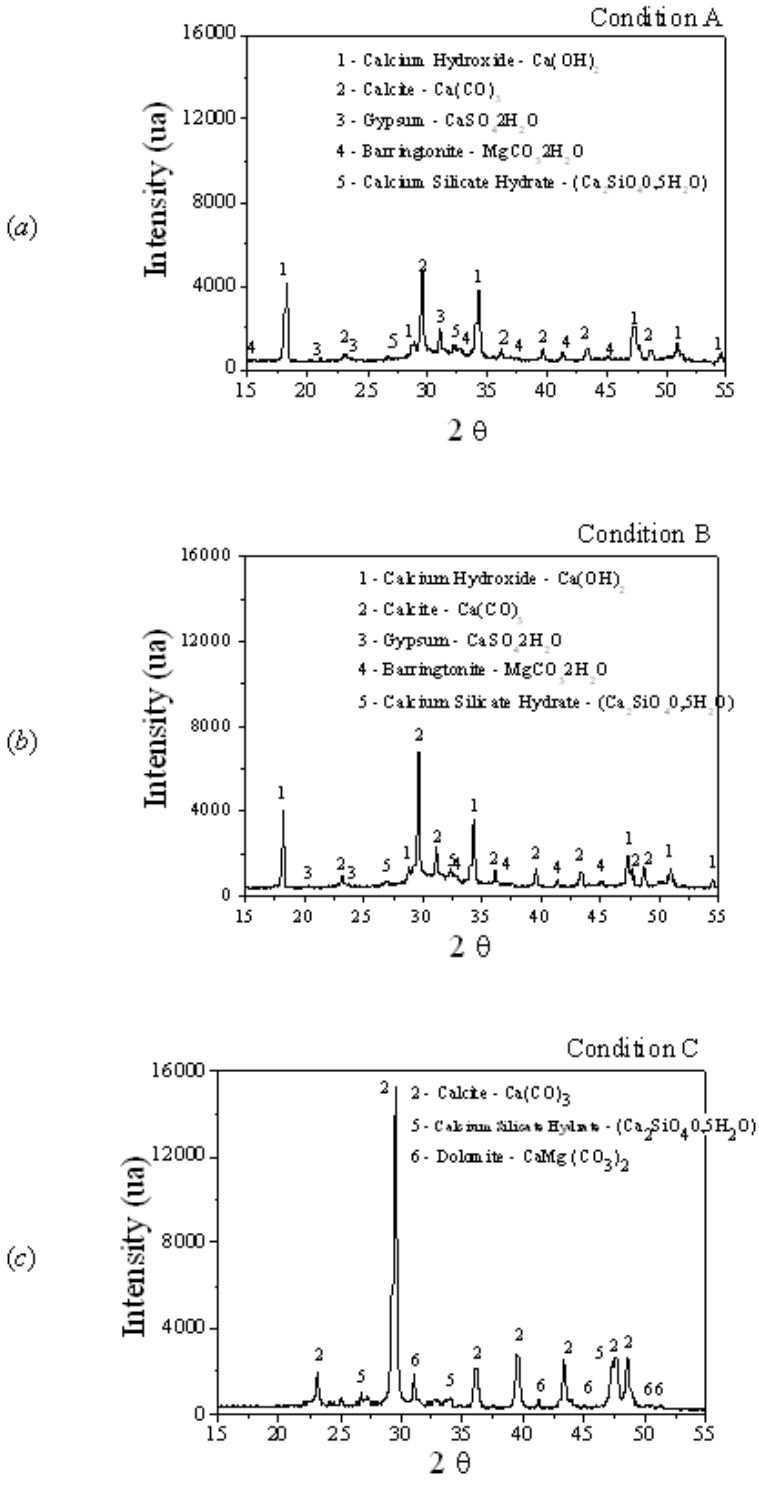

Figure 4. X-ray diffraction pattern of tiles: (a) non-aged (condition A), (b) after 100 ageing cycles (condition B), and (c) fast carbonated after 100 ageing cycles (condition C).

The cementitious phases of samples at each condition were analyzed by X-ray diffraction so that patterns in Figure 4(a) and (b) show the presence of calcium hydroxide, $Ca(OH)_2$, in samples not submitted to accelerated carbonation (conditions A and B). Conversely, $Ca(OH)_2$ was not identified in fast carbonated samples (condition C). The formation of greater amount of calcium carbonate instead of other carbonates can be associated to high percentage of calcium (about 60%) in the ordinary Portland cement used herein [39]. Such result suggests a successful CO_2 adsorption in the cement based matrix while high carbonation can be associated to the consumption of hydroxyls (OH) present within the cement matrix due to CO_2 adsorption after its diffusion into composite pores. High apparent porosity (AVV) of roofing tiles (around 44% at 28 days) contributed to such fast diffusion [40].

Series of accelerated carbonated roofing tiles after 100 ageing cycles (condition C) showed better mechanical performance in comparison to other series, including notably higher toughness (5.9 ± 1.9 kN·mm) and deflection at toughness (DTE = 9.1 ± 2.5 mm) in relation to non-aged (condition A) and fast-aged (condition B) series. The strength increase of aged material achieved in [41] was attributed to calcium hydroxide elimination due to carbonation treatment (109 days in a CO_2 incubator), mechanical performance improvement of flat sheets reinforced with 12% (mass basis) of Eucalyptus pulp after accelerated carbonation and ageing cycles was reported in [37].

In addition to chemical analysis, calcium carbonate ($CaCO_3$) microstructure in tile fracture surfaces was visualized via SEM - secondary electron (SE) images. In Figure 5 regarding fast carbonated tiles, one may observe $CaCO_3$ formation in crystals as well as packed in layers. As reported in [42], morphology of $CaCO_3$ crystalline state plays an important role in determining binder strength so that the improved strength was then attributed to the layered morphology of $CaCO_3$.

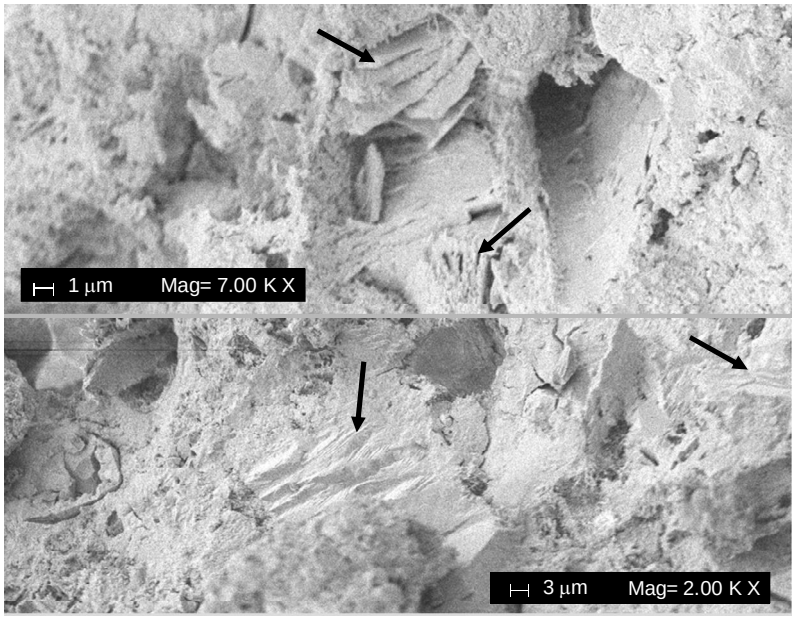

Figure 5. SEM of fracture surfaces of fast carbonated and aged tiles (condition C). Arrows indicate layered $CaCO_3$.

Last but not least, Figure 6 shows roofing tiles exposed to natural ageing. Such undulated shape is typically employed in Brazil.

Figure 6. Roofing tiles exposed to natural ageing in Brazil.

Thermal Properties of Undulated Tiles

Table 3 lists values for thermal conductivity k, specific heat c, and thermal diffusivity $\alpha = k/(\rho \cdot c)$ of composites, obtained by parallel hot wire method as described in [43]. Aforesaid thermal properties were determined at room temperature (i.e., 25°C) as well as at 60°C.

Table 3. Values for thermal conductivity k, specific heat c, and thermal diffusivity $\alpha = k/(\rho \cdot c)$ of composites, obtained by parallel hot wire method.

Mix design	Test temperature (°C)	k [W/(m·K)]	c [J/(kg·K)]	α (10^{-7} m^2/s)
Sisal fiber-cement (S4_7)	25	0.716	1278.7	3.060
	60	1.214	1071.5	6.191
Sisal + PP fiber-cement (S3PP1_7)	25	0.816	1201.1	3.951
	60	0.823	1294.4	3.694
Asbestos cement	25	0.837	1167.6	4.048
	60	0.967	1315.8	4.150

One notes that composites have different thermal behavior at room temperature (~ 25°C) and at 60°C. At the former, S4_7 formulation exhibited more favorable thermal properties for

thermal comfort, namely, lower thermal conductivity k and higher specific heat c, thus leading to lower thermal diffusivity α. At 60°C, formulation with PP fibers (S3PP1_7) presented more adequate values for thermal comfort. At both test temperatures, the mix-design with asbestos presented less appropriate values in comparison to the formulations without asbestos.

Raising test temperature to 60°C increased thermal conductivity and thermal diffusivity of composites with sisal (S4_7) up to 45% and 100%, respectively, compared to the other mix-design. One may point to the presence of moisture within prismatic specimens used to influence measurements, which may increase thermal conductivity for higher temperatures [44]. The fact that non-asbestos mix-design (S4_7) shows larger cellulose fiber content (thus presenting greater water absorption) may explain such thermal conductivity increase. Thermal behavior was also evaluated with respect to downside surface temperatures of non-asbestos roofing tiles produced (sisal fiber-cement – S4_7) compared with ceramic and asbestos-cement corrugated roofing sheets currently available in Brazilian market. Thermal behavior of roofing elements might also be influenced by product dimensions, shape, and color; however, a comprehensive discussion on those aspects is beyond the scope of the present chapter.

Thermal performance analysis of the roofing tiles considered the prospective influence of both cross-sectional area A and thickness Δx of the tile, its thermal conductivity k, and the temperature difference $\Delta T = T_{air} - T_{down}$, where T_{air} is the prevailing temperature of outside air while T_{down} is the downside surface temperature of the tile. Absolute values $dQ/dt = |\dot{Q}|$ for the heat transfer rate across the tile were calculated according to a one-dimensional approach of Fourier's law [45]:

$$\dot{Q} = -Ak\frac{dT}{dx} \quad \Rightarrow \quad \frac{dQ}{dt} = \left|Ak\frac{\Delta T}{\Delta x}\right| \tag{1}$$

At the hottest hours of the day, ceramics roofing tiles presented temperatures T_{down} up to 10°C lower than those of asbestos-cement sheets and 6°C lower in relation to those of sisal fiber-cement tiles. Among fiber-cement roofing tiles, non-asbestos tiles presented downside surface temperatures 3°C lower. Heat transfer resistance is directly related to the material microstructure (which can be assessed by its thermal diffusivity) and to its dimensions (mainly thickness) so that observed differences might be explained. Ceramic, non-asbestos, and asbestos roofing elements presented thicknesses around 12 mm, 8 mm, and 4 mm respectively. Heat transfer rates dQ/dt were calculated employing thermal conductivity data at 25°C as presented in Table 3 for fiber-cement tiles while literature values were assigned to ceramic tiles, namely, 1.05 W/(m·K) [46].

Solar radiation flux and heat transfer rate along different hours of the day are shown in Figure 7 for the hottest day over the evaluated period in summer. As one may see, heat transfer rates through asbestos-cement sheets were higher than rates related to ceramic and non-asbestos tiles. As a consequence, such higher rates lead to a hotter indoor environment. Related to the thermal diffusivity, thermal inertia is an important attribute for roofing tiles as it tends to reduce the amplitude of the thermal variation inside the building. For thermal inertia analysis, one may divide results into two periods, namely, morning and afternoon. In Figure 7, one observes that the highest radiation flux peak (about 1100 W/m^2) occurred at

10:00 am and at 11:30 am, whose effect was observed 1 h later with the increase of heat transfer rates through tiles. Ceramic tiles presented maximum heat transfer rate 15 min later than non-asbestos tiles and 30 min later than asbestos cement tiles, which can be attributed to the thermal inertia of the tiles. Furthermore, bearing in mind a barrier for thermal radiation, results suggested a better performance of ceramic and non-asbestos fiber-cement tiles.

In view of their lower heat transfer rates, sisal fiber-cement tiles rendered good capacity of lowering outdoor temperature peaks (more efficiently than asbestos fiber-cement ones). One may then claim resultant advantages concerning the reduction of thermal radiation penetration, which is a result in accordance to previous studies. Differences were found for sisal-reinforced fiber-cement roofing tiles (produced by vibration) around 11.5°C lower (at 12:00 pm) compared with asbestos-cement corrugated tiles [35] while significant differences were also observed for animal thermal comfort as the micro-environment of non-asbestos fiber-cement roofing tiles presented superior performance in relation to asbestos fiber-cement counterparts [47]. Employing fiber-cement roofing components based on blast furnace slag and vegetable pulps (Eucalyptus), differences of 7°C between internal and external surface temperatures were presented in [48].

Ceramic tiles showed slightly lower heat transfer rates compared to sisal fiber-cement ones, indicating a possible influence of tiles surface reflectance [49]. Although darker coloration of red ceramics tile suggests greater absorption (66%) in the visible spectrum, infrared reflectance is high enough (78%) to provide a total reflectance of about 67%. The opposite was observed for light gray non-asbestos fiber-cement tiles, with a total reflectance of approximately 40% [49].

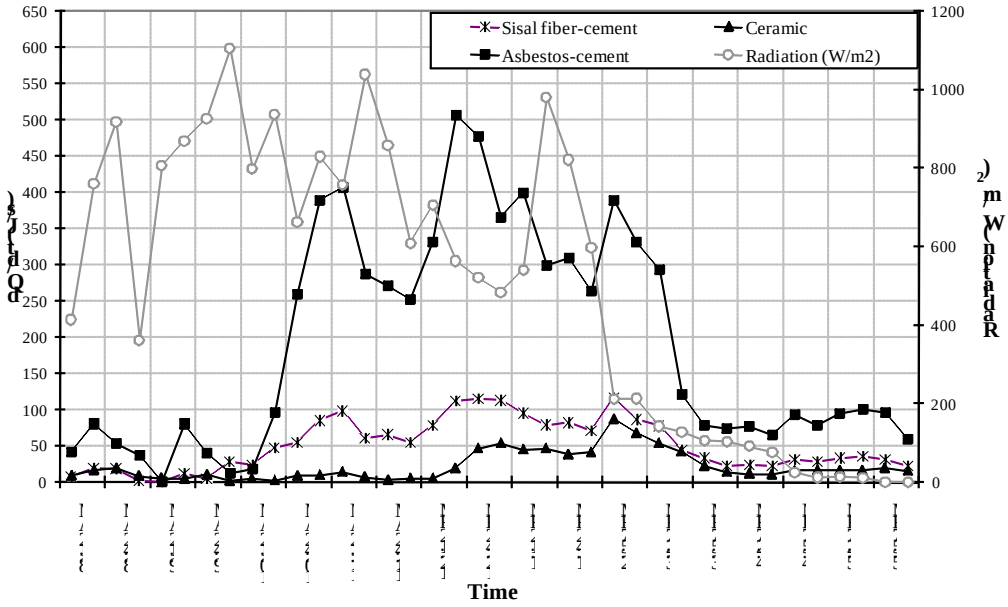

Figure 7. Variation of solar radiation and heat transfer rate through distinct roofing elements as a function of time. Data collected on December 22, 2005.

STRATEGIES FOR IMPROVING THE PERFORMANCE OF THE COMPOSITES

Flat composites were fabricated in order to evaluate the performance of the fiber-reinforced cement-based composites under various ageing conditions. Production method followed the slurry vacuum de-watering process aiming at the viable utilization of such materials in civil construction. Matrix materials were added to an appropriate amount of moist fibers pre-dispersed in water so as to form slurries within a 20-30% range (solid mass basis). After homogeneously stirred, slurry was immediately transferred to an evacuable box. Water was drawn off under vacuum until the pad appeared dry on the surface, whereupon it was flattened carefully with a tamper. Pads were then pressed at 3.2 MPa for 5 min and sealed inside a plastic bag for cure under saturated-air condition or water immersion for future mechanical tests at a total age of 28 days.

In some cases, further samples were prepared to evaluate their performance after natural or accelerated ageing experiments. Tests were carried out so as to evaluate prospective effects due to (*i*) matrix modification by less alkali blends, (*ii*) different fiber contents, (*iii*) decrease of fiber mineralization by chemical modification, (*iv*) improvement of fiber-to-cement bonding, and (*v*) decrease of the distance between fibers. Related results are presented and discussed in the sequence.

Effects due to Matrix Modification by Less Alkali Blends

In order to improve the durability of the composites, diminution of the matrix alkalinity was attempted. The main component to produce the paste matrix was the alkaline granulated iron blast-furnace slag (BFS) ground to 500 $m^2 \cdot kg^{-1}$ Blaine fineness, presenting the following oxide composition (mass-basis) as provided in [50]: SiO_2 - 33.78%, Al_2O_3 - 13.11%, Fe_2O_3 - 0.51%, CaO - 42.47%, MgO - 7.46%, SO_3 - 0.15%, Na_2O - 0.16%, K_2O - 0.32%, free CaO - 0.10%, and CO_2 - 1.18%. In Brazil, more than 6 million tons of basic ground-BFS (GBFS) are available every year, generated by the steel industry [51]. GBFS costs can be as low as USD 10.00 per ton.

For the cement production, slag must be ground to fineness at least similar to that of the ordinary Portland cement, which adds a further cost of approximately USD 15.00 per ton, and it must be activated by alkaline compounds. Gypsum for agricultural purposes and lime (calcium hydroxide) for civil construction were elected as chemical alkali-activators for BFS respectively in proportions of 10% and 2% (binder mass basis), as discussed in [52]. Standard commercial ordinary Portland cement (OPC), Adelaide Brighton brand type "general purpose" (GP), minimum compressive strength of 40 MPa at 28 days (Australian Standards AS 3972 and AS 2350.11) was adopted as the reference matrix to compare with BFS cement.

As detailed in [14], waste strand fibers generated during crop stages of both sisal (*Agave sisalana*) and banana (*Musa cavendishii - nanicao* cultivar) were initially cut to around 30 mm in length. Via filtration from drainage lines prior to effluent biological treatment, waste *Eucalyptus grandis* pulp from Kraft and bleaching stages was also collected (at about 0.5% by mass) from a commercial production of a cellulose mill.

Aiming at cheaper price and economical viability at small-scale production (if compared with chemical pulps), strand fibers underwent low-temperature chemithermomechanical pulping (CTMP) in line with [53], [54]. Additionally mechanical beating provided important internal and external fibrillation of filaments, leading to conformable fibers and thus to fiber-matrix bonding improvement. Initial preparation comprised soaking in cold water overnight, followed by simple and low-pollutant chemical pre-treatment based on 1-hour cooking in boiling saturated lime liquor. Such step effectively attacked residual slivers, which could be easily broken by fingers, thus showing adequate preparation for subsequent mechanical treatments. Appropriate chemical attack is of utmost importance for reducing energy consumption, which represents one of the major concerns related to mechanical pulps [6]. Some pulp and fiber properties are summarized in Table 4.

Table 4. Some pulp and fiber properties of interest.

Fiber	By-produced sisal CTMP [f]	Banana CTMP [f]	*E. grandis* Kraft waste
Screened yield (%)	43.38	35.57	N/A
Kappa number [a]	50.5	86.5	6.1
Freeness (mL) [b]	500	465	685
Length-weighted average length (mm) [c]	1.53	2.09	0.66
Fines (%) [d]	2.14	1.55	7.01
Fiber width (μm) [e]	9.4	11.8	10.9
Aspect ratio	163	177	61

[a] Appita P201 m-86 [55]; [b] AS 1301.206s-88; [c] Kajaani FS-200; [d] Arithmetic basis; [e] Average from 20 determinations by SEM; [f] Chemithermomechanical pulping (CTMP); N/A: not available.

Asplund laboratory defibrator provided 103 kPa steam gauge pressure corresponding to 121°C in presence of the pre-treatment solution with pre-steaming by 120 s and defibration by additional 90 s. At those conditions [6], well fibrillated softwood fibers could be obtained from low temperature (i.e., 125-135°C) CTMP instead of yield smooth, lignin encased and un-fibrillated fibers from high temperature (i.e., 150-175°C) pulping. The pulp in preparation passed through a Bauer 20 cm laboratory disc refiner equipped firstly with straight open periphery plates (1 pass at 254 μm clearance) and subsequently with straight closed periphery plates (1 pass at 127 μm and 1 pass at 76 μm). Partial de-watering before each refinement step provided pulp with adequate consistency for the improvement of the defibration process.

Sisal and banana pulps passed through a 0.229 mm slotted Packer screen for separation of shaves and then through a supplementary Somerville 0.180 mm mesh screening and subsequent washing to reduce particles with length below 0.2 mm. Fibers shortening and fines generation are expected although undesirable results from beating procedures can be controlled via appropriate energy applied to the stock during the mechanical treatment [53]. Finally, the produced pulps were vacuum de-watered, pressed, crumbed, and stored in sealed plastic bags under refrigeration. *Eucalyptus grandis* waste pulp was employed just as received

after a 2 min disintegration and washing in hot (nearly boiling) water using a closed-circuit pump system.

Figure 8 shows results from mechanical and physical tests on composites reinforced with 8% of produced sisal and banana pulps as well as with waste *Eucalyptus grandis* pulp from Kraft and bleaching stages. Flexural strength around 18 MPa for 8% residual fiber-BFS composites is considered an acceptable achievement when using mechanically pulped fibrous raw materials in comparison with similar results [54] for sisal Kraft pulp as reinforcement of air-cured BFS based matrices in 17 MPa and 1.4 $kJ \cdot m^{-2}$ ranges for flexural strength and toughness, respectively. Current results may also be considered a significant advance over a previous work [56] using disintegrated paper reinforced OPC with flexural strength up to 7 MPa at least 30% less than the corresponding control matrix under dough mixing method for fabrication.

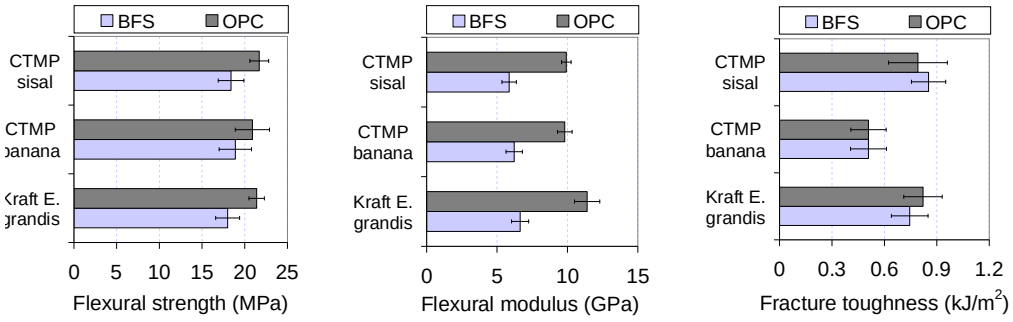

Figure 8. Average values and standard deviations for mechanical properties of composites as a function of the type of pulp fibers and matrix.

OPC-based composites performed superior mechanical strength around 21 MPa at 28 days of age associated to lower water absorption in comparison to BFS composites with all tested fibers in 8% content. BFS matrix seemed to lack hydration improvement, which could be achieved by high-temperature cure up to 60°C [57] or by adopting another alkaline activator (e.g., sodium silicate) as proposed in [58].

The high standard deviation associated with the flexural strength could be justified by the heterogeneity of the reinforcement fibers based on the following facts:

- Fibrous wastes generally present high moisture content and are thus expected to undergo fast biological decay [59], [60], leading to weak fibers in the pulp;
- Mechanical refinement often originates bunches of individual fibers mutually linked by non-cellulose compounds (e.g., lignin), as indicated in Table 4 by high Kappa numbers for sisal and banana CTMP. Strand fibers thus tend to perform poor distribution in the cement matrix.

BFS composites reinforced with banana fiber showed lower values for fracture toughness compared to both sisal and *Eucalyptus grandis* composites. It is a result of high length and aspect ratio of banana fiber, which leads to a stronger anchorage in the matrix and to the predominance of fiber fracture during mechanical test before any further fiber displacement

could occur, as depicted in Figure 9(*b*). Figures 9(*d*) and 9(*e*) show images of by-product sisal CTMP in OPC with the desirable coexistence between fractured and pulled out filaments, pointing to the proximity of critical length [61] of that fiber in the specified matrix under ambient moisture condition. Twisted and bent fibers reinforce the idea of optimum interaction between both phases as well as of high energy dissipation during fiber pullout. Such favorable microscopic behavior explains the suitable compromise between flexural strength (21.7 MPa) and toughness (0.792 $kJ \cdot m^{-2}$) for 8% sisal CTMP in OPC (Figure 8).

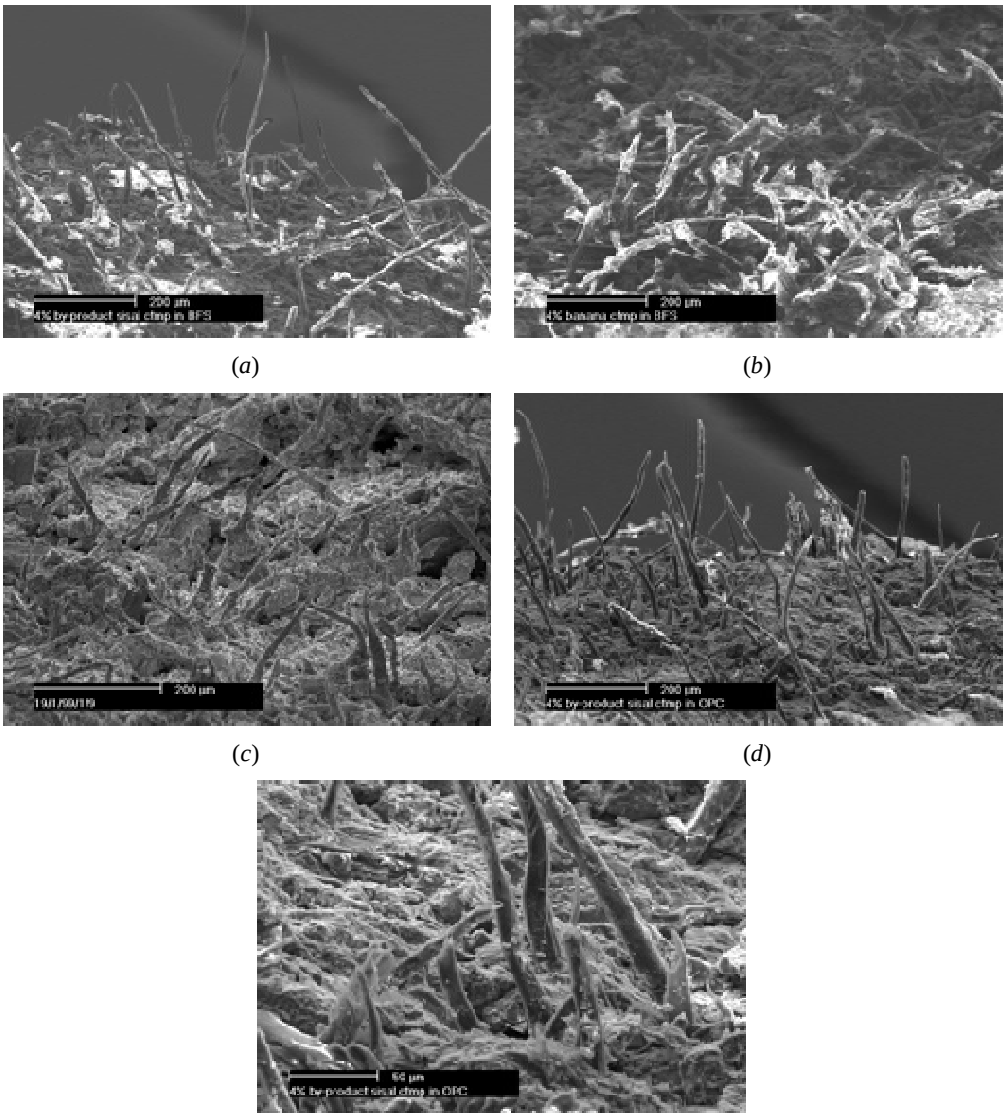

(*a*) (*b*)

(*c*) (*d*)

(*e*)

Figure 9. Sequence of scanning electron microscope (SEM) images (hydration age between brackets): (*a*) 4% sisal CTMP in BFS matrix (73 days); (*b*) 4% banana CTMP in BFS matrix (32 days); (*c*) 4% *Eucalyptus grandis* waste Kraft in BFS matrix (51 days); (*d*) 4% sisal CTMP in OPC matrix (67 days); (*e*) 4% sisal CTMP in OPC matrix - higher magnification (67 days).

Freeness values within 465- 685 mL range (Table 4) provide adequate water drainage and prevent cement particles loss during suction stage of industrial systems based on Hatschek model for panels fabrication as pointed in [62], [63]. Low Kappa number value (Table 4) for *Eucalyptus grandis* Kraft pulp is an indication of bleached fiber with low lignin content. On the other hand, high values for mechanical pulps suggest damaged and fibrillated filaments or even remaining slivers expected to present exposed lignin to undesirable alkaline attack inside cement matrices.

As also concluded in similar research [64], [54], density, water absorption, and porosity are interrelated properties. Low densities are preferable to reduce transportation costs and carriage effort while they are normally connected to higher water absorption values with the inconvenient increase of the self-bearing load during utilization and to risk of excessive permeability. As a reference, Brazilian standards (NBR 12800 and NBR 12825) limit water absorption to 37% (mass basis) for fiber-cement corrugated roofing sheets.

Elevated presence of fines in waste *Eucalyptus grandis* Kraft (Table 4) could contribute to packing effect inside cement matrices, thus leading to denser materials with lower water absorption and apparent porosity, if compared to other OPC and BFS composites for the same fiber content (Figure 10). Such observation is consistent with results from wastepaper fiber-cement composites research reported in [65].

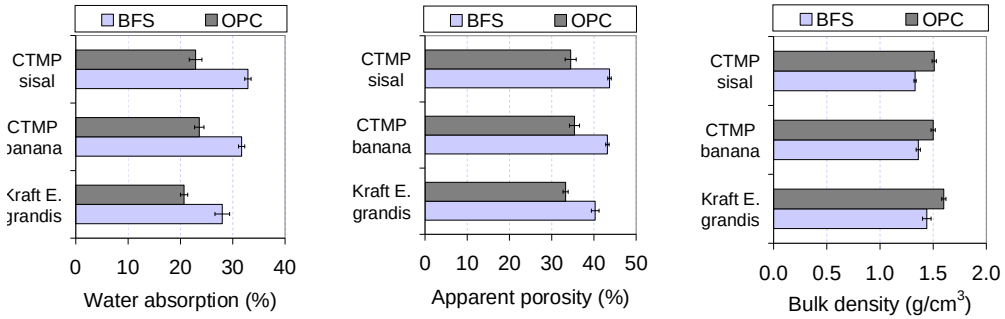

(*a*) (*b*) (*c*)

Figure 10. Average values and standard deviations of the physical properties of the composites in function of the type of pulp fibers and matrix.

Effects due to Different Fiber Contents

Figure 11 and Figure 12 present the effect of the fiber content respectively on mechanical and physical performance of composites. The formulations follow those for BSF composites as presented in the previous section, except for variable fiber content. All BFS composites showed a considerable increase (at least 20%) in flexural strength within the 8-12% fiber content interval if compared to the corresponding 4% fiber content composites (Figure 11).

The short length of *Eucalyptus grandis* (Table 4) allowed the inclusion of up to 16% of fiber by binder mass although losing flexural strength, which could be associated to the high volume of permeable voids. As *Eucalyptus grandis* fiber content increased from 4% to 16%, the elastic modulus in bending of BFS composites decreased from 9 GPa to 4 GPa, a behavior that was equally observed for the other similar fiber-cements. Materials with 8% fiber OPC

showed significantly higher modulus than corresponding BFS ones, likely due to insufficient hydration attributed to the BFS binder as previously commented.

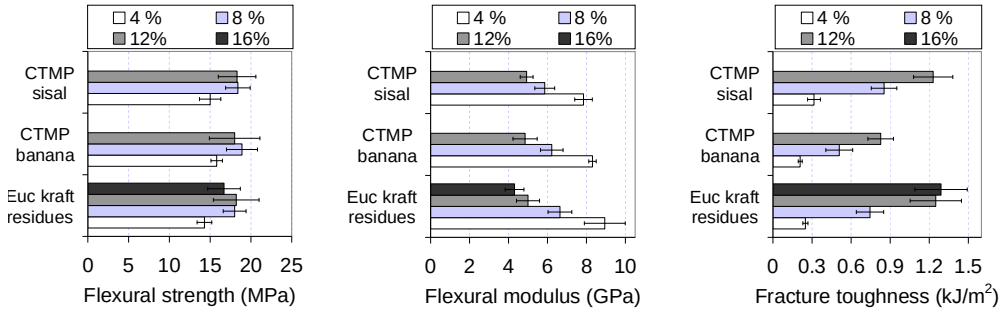

(*a*) (*b*) (*c*)

Figure 11. Variation of mechanical properties as a function of fiber content (%, mass basis) for composites with different pulp fibers.

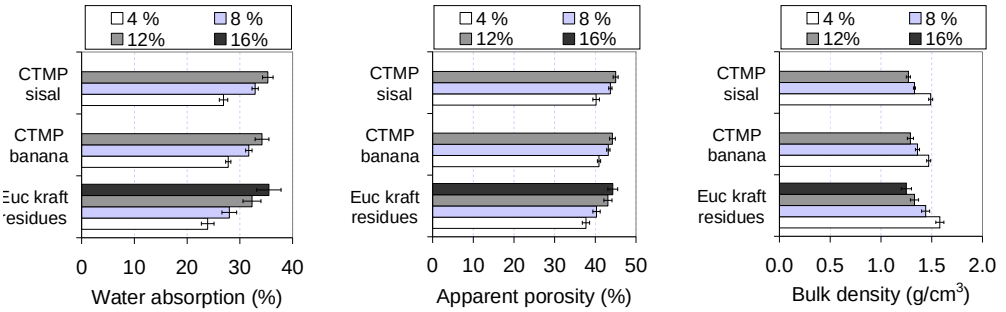

(*a*) (*b*) (*c*)

Figure 12. Variation of physical properties as a function of fiber content (%, mass basis) for composites with different pulp fibers.

The fracture toughness was greatly enhanced up to 5-fold by fiber reinforcement from 4 to 12% load interval. As observed in Figure 11(*c*) for *Eucalyptus grandis* BFS composites, best energy absorption seems to fall between 12 and 16% of fiber content with toughness in the vicinity of 1.3 $kJ \cdot m^{-2}$. Predominance of fiber pullout for sisal and *Eucalyptus grandis* composites (see Fugures 9(*a*) and 9(*c*)) is related to the high frictional energy absorption. In the specific case of *Eucalyptus grandis* fibers, the short length is compensated by larger number of filaments for a fixed fiber content and, hence, by higher probability of matrix micro-crack interception in its initial stage of propagation. Increase of fiber content leads to poor packing during composites preparation, especially at the pressing stage. Cellulose fibers are highly conformable and play a spring effect inside the cement matrix immediately after the press release. Owing to compaction reduction in combination with fibers of low bulk density (~ 1,500 $kg \cdot m^{-3}$) and high water absorption, permeable voids volume and water absorption increase linearly with fiber content.

Effects due to Decrease of Fiber Mineralization by Chemical Modification

Eucalyptus Kraft pulp fibers were submitted to chemical treatment in order to reduce their hydrophilic character. The procedure for surface treatment of Eucalyptus pulp fibers and the option for silanes were based in studies as developed in [66]. The silanes employed were methacryloxypropyltri-methoxysilane (MPTS) and aminopropyltri-ethoxysilane (APTS), in a proportion of 6% by mass of cellulose pulp. Silanes were pre-hydrolyzed during 2 h under stirring in 80/20 volume basis ethanol-distilled water solution. Cellulose pulp was introduced (5% by mass basis) followed by further 2 h of stirring. Composites were prepared by the same procedure as described in the previous section, using 5% by mass of (untreated or treated) pulp in a matrix composed by 85% of OPC and 15% of carbonate filler.

Effect of treating pulp fibers on their mineralization was analyzed using scanning electron microscope (SEM) and back-scattered electron (BSE) detector to view cut and polished surfaces. BSE images allow easy identification of composite phases via atomic number contrast. Figure 13 presents SEM micrographs of composites whose pulp fibers are either impregnated with or free from silane coupling agents, where black areas are cross-sections of pulp fibers. In composites with untreated and APTS treated pulp fibers, Figures 13(*a*) and 13(*b*) respectively, one observes that the majority of lumens were filled up with reprecipitated products from cement hydration, while in composites with MPTS treated pulp fibers, Figure 13(*c*), fiber lumens are free from hydration products.

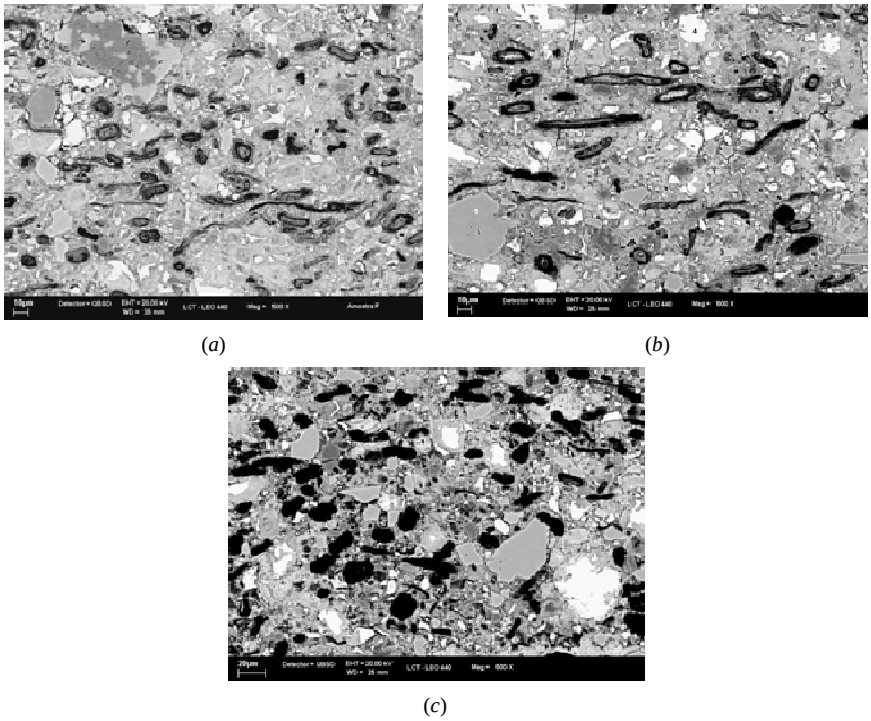

(*a*) (*b*)

(*c*)

Figure 13. SEM-BSE images of composites reinforced with Eucalyptus bleached pulps: (*a*) untreated, (*b*) APTS treated, and (*c*) MPTS treated (after 200 ageing cycles).

Table 5 shows the effect of pulp treatment on the mechanical performance of composites. At 28-days cure, composites with APTS silaned pulp presented significantly higher modulus of rupture (MOR) than composites with untreated pulp or MPTS silaned pulp whereas toughness of the composites was not influenced by silane treatment. Similar results for composites reinforced with silane-treated fibers were found in [67], [68].

Table 5. Average values and standard deviations for properties of composites: limit of proportionality (LOP), modulus of rupture (MOR), modulus of elasticity (MOE) and toughness (TE).

Fiber treatment	Condition	LOP (MPa)	MOR (MPa)	MOE (GPa)	TE (kJ/m^2)
Untreated	28 days	6.9 ± 1.1	9.9 ± 1.4	13.3 ± 1.2	0.86 ± 0.25
MPTS		6.5 ± 1.0	10.7 ± 1.3	16.3 ± 1.7	0.83 ± 0.46
APTS		7.8 ± 1.3	12.1 ± 1.4	16.3 ± 2.5	0.82 ± 0.29
Untreated	200 cycles	6.3 ± 0.9	7.5 ± 0.5	17.7 ± 1.1	0.13 ± 0.07
MPTS		7.2 ± 0.9	8.0 ± 1.0	18.6 ± 4.6	0.30 ± 0.12
APTS		6.9 ± 1.7	8.3 ± 1.0	18.4 ± 3.8	0.13 ± 0.07

Average MOR values notably decreased after 200 ageing cycles for composites with either treated or untreated fibers compared to those after 28 days cure. MOR differences after ageing were not observed between composites with treated or untreated fibers. As suggested in Table 5, the fact that MPTS-treated pulp did not present fibers filled up with products from cement hydration seems to influence the higher toughness of the corresponding composites after 200 ageing cycles. Yet, for untreated and APTS-treated pulps, composite capacity to absorb energy was markedly decreased most likely due to reprecipitation of hydration products into fibers permeable voids with consequent composite embrittlement.

Table 6. Average values and standard deviations for properties of composites: water absorption (WA), apparent void volume (AVV), and bulk density (BD).

Fiber treatment	Condition	WA (%)	AVV (%)	BD (g/cm^3)
Untreated	28 days	16.4 ± 0.9	29.0 ± 1.0	1.77 ± 0.04
MPTS		17.7 ± 1.3	30.8 ± 1.5	1.75 ± 0.04
APTS		16.7 ± 0.8	29.9 ± 1.0	1.79 ± 0.03
Untreated	200 cycles	15.2 ± 1.2	26.5 ± 1.9	1.75 ± 0.03
MPTS		16.2 ± 1.7	27.9 ± 2.4	1.72 ± 0.08
APTS		13.5 ± 0.5	24.6 ± 0.7	1.83 ± 0.03

The effect of silane treatment on composites physical properties is presented in Table 6. Significant differences were not observed between composites with treated or untreated pulp at 28 days. However, after 200 ageing cycles, composites with APTS-treated pulp presented

lower water absorption and apparent porosity in relation to composites with untreated pulp and MPTS-treated pulp. Bulk density of composites with APTS-treated pulp was significantly higher after 200 ageing cycles. This behavior suggests that chemical treatment increased the interaction with cement, which influenced physical properties of the composite. Lower porosity of composites reinforced with silaned carbon fibers was reported in [69]. In such study, authors attributed this behavior to the hydrophilic character of the silane used, which improved fiber-matrix bond. The fact that fibers are filled up with cement hydration products also explains the porosity decrease of composites.

The chemical composition of virgin pulp fibers seems to exert significant influence on composites durability as well. Lignin is an amorphous chemical species with high solubility in alkaline medium and its removal is essential part of pulping process [4]. Further lignin extraction from pulps is normally referred to as bleaching treatment. Figure 14 presents the influence of bleaching Eucalyptus pulp fibers in order to improve adhesion between fibers and matrix. Bleaching process makes fiber more susceptible to mineralization as it extracts compounds from fiber cell wall structure.

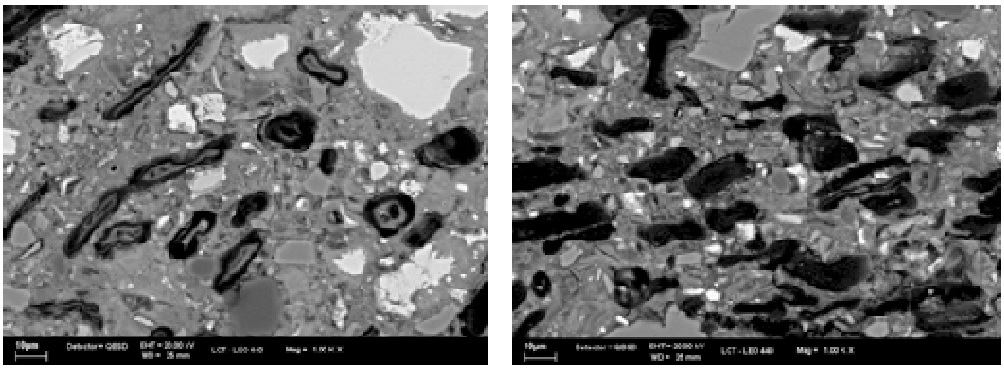

(*a*) (*b*)

Figure 14. SEM-BSE images of composites reinforced with Eucalyptus: (*a*) bleached and (*b*) unbleached (28 days).

Effects due to Improvement of Fiber-to-Cement Bonding

One possible treatment to enhance mechanical performance of composites reinforced with cellulose pulp is the refining process, which is carried out in the presence of water, usually by passing the suspension of pulp fibers through a disc refiner composed by a relatively narrow gap between rotor and stator [70], [71]. Cellulose fibers are intrinsically strong and refinement improves their ability to be processed, which is necessary if the composite is manufactured using Hatschek production method [72]. The main effect of refinement in cellulose fiber structure as a result of mechanical treatment is the fibrillation of fibers surface [73]. These fibrillated and short fibers are responsible for the formation of a net inside the composite mixture with the consequent retention of cement matrix particles during de-watering stage of manufacturing process. Better fiber-matrix interface adhesion and mechanical performance can be achieved by increasing the specific surface area of the fiber,

by reducing the fiber diameter and producing a rough surface proportioning better mechanical anchorage in the matrix [72].

Figure 15(*a*) presents the poor adhesion of unrefined sisal pulp fibers and depicts void sizes up to 3 μm at the interface between fiber and matrix. In composites with refined pulp fibers, external layers were partially pulled out from cell wall after refining and these external layers then improve fibers anchorage into the cementitious matrix. In Figure 15(*b*), one may see external layers of refined fibers largely bonded to the cementitious matrix. The refined fiber-cement paste bond seems to be stronger than the unrefined fiber-cement paste bond, as asserted in [74]. The large superficial contact performed by refined cellulose pulp has enhanced the mechanical performance and has improved the load transfer from matrix to fibers [75].

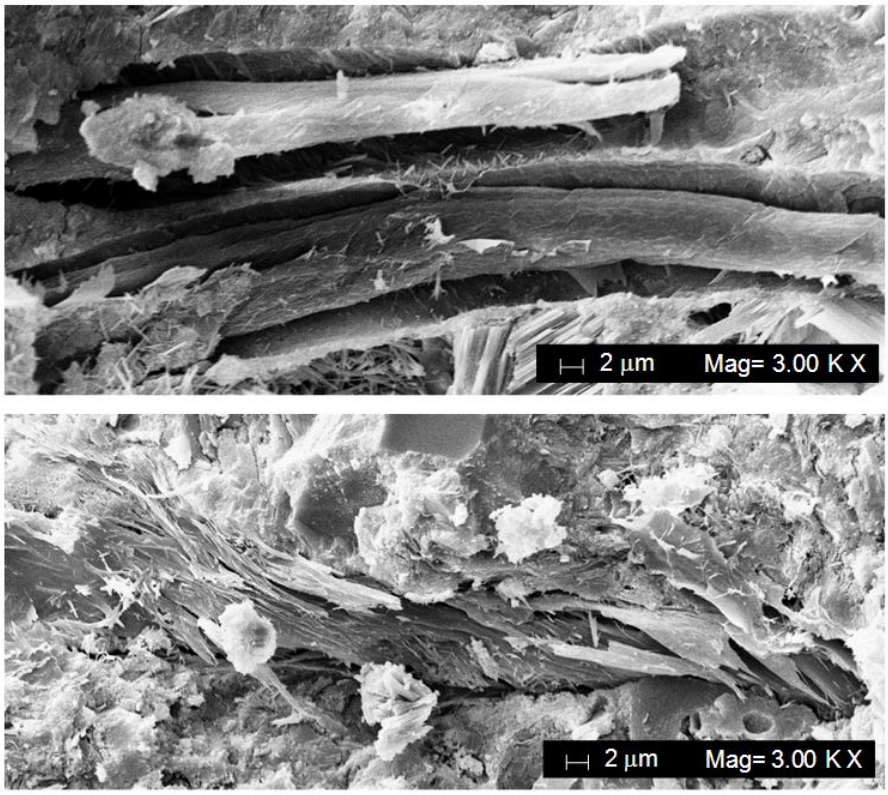

Figure 15. SEM micrographs of fractured surfaces of sisal fiber-cement composites with (*a*) unrefined pulp (CSF 680 mL) - voids at the fiber-matrix interface after 100 soak / dry ageing cycles; (*b*) pulp refined at CSF 20 mL and after 100 soak / dry ageing cycles.

The state of the surface structure of vegetable pulp fibers may vary due to their natural source or due to the pulping process. Roughness of unrefined and unbleached Eucalyptus and Pinus pulps were evaluated via atomic force microscopy (AFM). The surface of Eucalyptus fibers presented some fibrillar structure in most samples (arrow in Figure 16(*a*)). In Pinus fibers, typical surface structure was granular (arrow in Figure 16(*b*)), possibly related to amorphous non-carbohydrates (lignin and extracts) in the fiber surface. Fibrillar surface

structures of Eucalyptus fibers suggest a higher potential for Eucalyptus fibers to anchorage in the cement matrix.

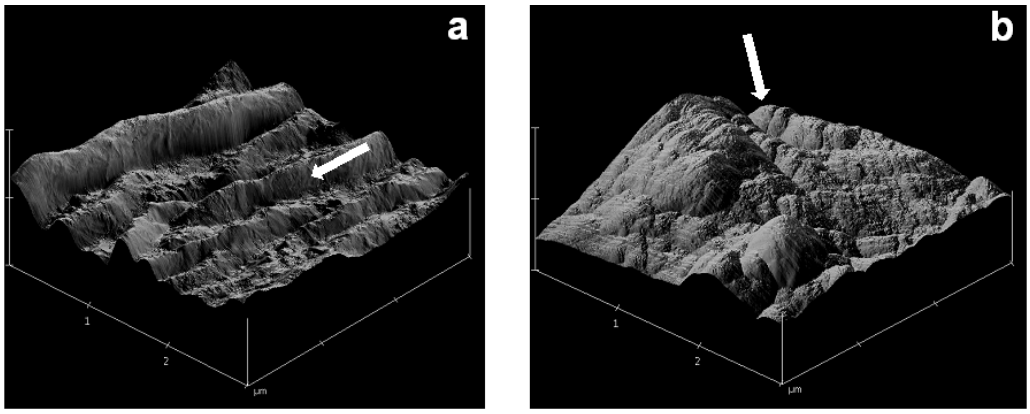

(*a*) (*b*)

Figure 16. AFM topography images of (*a*) unbleached Eucalyptus fibers and (*b*) unbleached Pinus fibers. Image sizes are 3 µm × 3 µm; m; vertical axis in the images is 500 nm long.

Similar to the procedure previously cited, the interface between pulp fibers and cement matrix was analyzed utilizing SEM-BSE. In composites cross-sections after accelerated ageing cycles, arrows in Figure 17 show improved interface of (*a*) Eucalyptus fibers compared with (*b*) Pinus fibers.

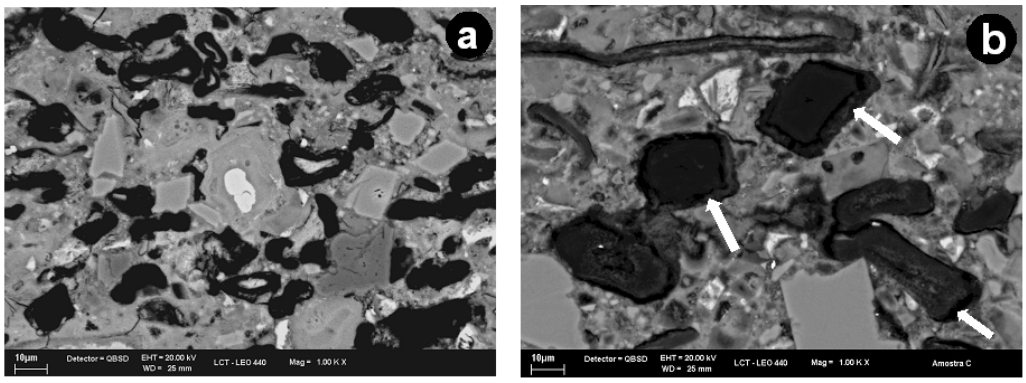

(*a*) (*b*)

Figure 17. SEM-BSE image of composites reinforced with (*a*) Eucalyptus pulps and (*b*) Pinus pulps, after accelerated ageing.

A subsequent mercury intrusion porosimetry (MIP) analysis evidenced a higher content of larger pores (withn the 1000-3000 nm range) in composites reinforced with Pinus fibers, as shown in Figure 18. One might then attribute such result to voids in the corresponding fiber-matrix interface.

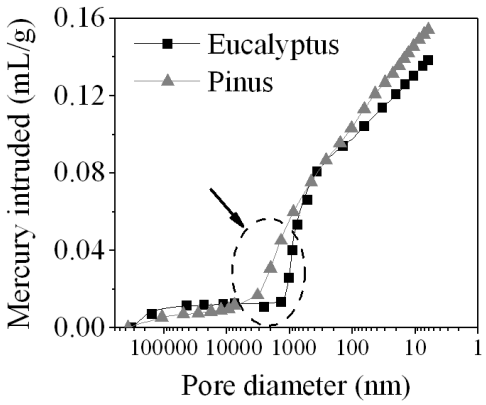

Figure 18. Composites reinforced with Eucalyptus and Pinus pulps: corresponding cumulative mercury intrusion porosimetry (MIP) analysis.

Effects due to Decrease of the Distance Between Fibers

Mechanical properties of fiber-cement composites are very sensitive to the uniformity of fibers volume distribution (dispersion) whereas the distance (spacing) between fibers is a critical geometrical parameter for composites performance [76]. As a rule, cracks initiate and advance from a composite section that has larger fiber-free matrix regions and fiber clumping [77]. Crack initiation requires less energy if it increases the size and the number of matrix regions that are not reinforced by fibers and such phenomenon becomes more pronounced in view of the progressive cement matrix embrittlement throughout its ageing.

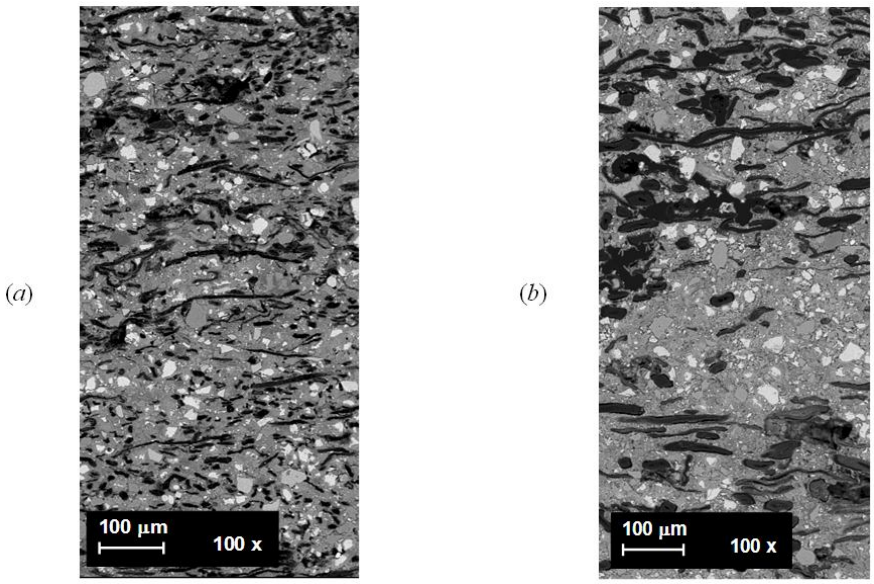

Figure 19. SEM-BSE image of composites reinforced with (*a*) Eucalyptus pulp and (*b*) Pinus pulp.

Likely to be more homogeneous in length, Eucalyptus pulp presents shorter fibers (0.83 ± 0.01 mm) than Pinus pulp (2.40 ± 0.09 mm). As the use of short fibers might lead to higher number of fibers per volume or weight in relation to long fibers, the former may reduce fiber-free areas, i.e., the distance between fibers. Additionally, the smaller the fiber length is (which usually refers to lower aspect ratio), the easier the fiber dispersion becomes [78].

Comparing Figures 19(*a*) and 19(*b*), short Eucalyptus fibers are better distributed than Pinus fibers. Bridging fibers share and transfer the load to other parts of the composite, which increases composite MOR and toughness. Calculated fiber spacing is at least two times higher for Pinus fibers relative to Eucalyptus ones [76]. Furthermore, due to their longer length, fibers in Pinus pulp are prone to cling to one another, thus jeopardizing the reinforcement.

PHOSPHOGYPSUM: RADIOLOGICAL CONCERNS AND PERFORMANCE

In line with the agricultural boom experienced during the past decades, Brazilian demands for phosphate fertilizers have increased accordingly. As a consequence, considerable amounts of phosphogypsum have been by-produced, whose large-scale exploitation as a non-conventional building material has challenged and motivated many research lines. Difficulties to be overcome refer not only to the constructive aspects but also to the radioactively safe use of phosphogypsum in substitution of ordinary (i.e., commercial) gypsum. With respect to the environmental issue related to this agricultural waste, concerns are addressed to radon-222 (^{222}Rn) exhalation from phosphogypsum-bearing building materials

Most of the total radiation received by humans has to do with ^{222}Rn, which is a decay product from uranium, actinium, and thorium. As such radioactive noble gas can naturally occur in soil formations, it can penetrate into dwellings through microscopic cracks in the building structure. Exposure risks to inhabitants can equally be attributed to ^{222}Rn exhaled from building materials themselves, in which case phosphogypsum-bearing materials are likely to fall. Belonging to ^{238}U decay chain, ^{222}Rn results from α-decay of ^{226}Ra, which is an impurity frequently observed in phosphogypsum. Hence, ^{226}Ra trapped in phosphogypsum-bearing materials eventually decays to ^{222}Rn and such gaseous radionuclide may percolate the porous matrix, reach up open air (local atmosphere or indoor air), and be eventually inhaled by nearby humans or animals.

Radon exposure belongs to the scope of environmental toxicology and its exhalation rate closely depends on the prevailing distribution in the porous medium. Research has been conducted in order to measure and correlate those rates to known physical parameters regarding the porous medium such as emanation rates from ^{226}Ra, moisture content, grain size, porosity, permeability, species (^{222}Rn) diffusivity, and temperature [20].

Though radiological issues concerning phosphogypsum management still remain, there is a broad interest in finding its large-scale exploitation. Accordingly, besides the constructive performance viewpoint, the use of such agroindustrial waste as a substitute for ordinary gypsum deals with ^{222}Rn exhalation. Comprehensive understanding of ^{222}Rn generation and its transport can be useful to assess related radiation exposure, to set up acceptable radiological standards, and to devise radiological protection based on human health threats.

MODELING AND SIMULATION OF RADON-222 EXHALATION

Similar to several other applications [79], [80], ^{222}Rn exhalation from phosphogypsum-bearing materials involves transport phenomena in porous media. Besides diffusion and convection, ^{222}Rn accumulation in dwellings can be concurrently affected by emanation (from ^{226}Ra), adsorption, absorption, and self-decay [81], [82]. Initial model frameworks have considered diffusion and convection with interstitial air flow driven by prescribed pressure differences in line with Darcy's law [83], [84], [85], [86]. Including pressure fluctuations [87], such approach has been adopted until lately [88] as it yields a Poisson equation (for transient transport) or a Laplace equation (for steady-state transport) to be solved for pressure, which simplifies the numerical implementation of governing equations into a computational code[4]. Including entry rates from water and building materials, a steady-state balance for indoor ^{222}Rn concentration was proposed in [89] whereas a transient model for exposure to phosphogypsum panels was recently presented in [90]. Further theoretical contributions comprise transient models for ^{222}Rn diffusion and decay in activated charcoal [91] and for ^{222}Rn and ^{210}Pb transport through the atmosphere [92].

Accounting for sources (e.g., from distinct building materials [22]), time-dependent model frameworks have attempted to assess ^{222}Rn entry rates and its accumulation inside building or enclosures based on bulk values. With respect to spatial coordinates, such models are forcibly of zero-order so that indoor ^{222}Rn concentration is allegedly uniform throughout the entire domain. Whenever point-to-point variation must be analyzed, failure of zero-order approaches is expected because they solely provide volume-averaged ^{222}Rn concentrations. Detailed ^{222}Rn indoor distributions can only be achieved by means of higher order model frameworks in space [93].

Comprehensive models for indoor-air ^{222}Rn exhalation and accumulation become stiffer as more and more influencing processes are entailed. Experimental data do help to asses and depict real and complex behavior but field or laboratory data acquisition might be risky or should be avoided due to safety concerns, technological constraints, or economic issues (costly human or material resources). Since such situation is applicable to the alternative use of phosphogypsum, numerical simulation may then play an important role by rapidly (and safely) investigating any prospective scenario, evoking as few simplifying assumptions as possible while accounting for effects sometimes conveniently neglected or simply ignored.

Nuclear physicists or engineers may rely on simulation if, for instance, non-linear and/or transient behavior, three-dimensional domains, or irregular geometry should be analyzed. Such real-world problems (for which computational time was prohibitive years ago) may help one to define proper radiological protection standards or design. A finite-difference method to predict ^{222}Rn entries into house basements from underneath soil gas was implemented following Darcy's law in [84] while a simulator for ^{222}Rn transport in soil was developed in [86]. Assuming air flow driven by user-defined pressure differences, a finite-volume method code was developed in [88] including time variation, three-dimensional domains, and several controlling parameters whereas fluctuations in such driving pressure differences were numerically investigated in [87].

[4] Otherwise, one should additionally evoke and solve complete (and stiffer) momentum equations.

Modeling ^{222}Rn Exhalation from Phosphogypsum-Bearing Materials: Primitive Variables

A porous medium is a solid matrix with an interconnected void system (i.e., interstices) through which fluids may flow [79]. If only one fluid saturates the void space, single-phase flow occurs; in a two-phase flow liquid and gaseous phases share the interstices [80]. Macroscopic measurements are normally achieved on regions or samples comprising several pores so that space-averaged physical quantities are assumed to continuously vary on time and on spatial coordinates. Porosity ε of a medium is a dimensionless quantity measuring the total volume fraction occupied by void space and such definition takes for granted that interstices are in fact connected. A basic concept behind such average is the representative elementary volume (REV), whose characteristic length is much larger than the pore scale but significantly smaller than the macroscopic domain length. Governing equations are derived for quantities at REV center and resulting values are allegedly independent from REV size. A REV in phosphogypsum-bearing porous materials may contain solid grains (or lattice) as well as pore space filled with air and/or water (for wet conditions) so that its porosity ε may encompass both air-based ε_a and water-based ε_w counterparts ($\varepsilon = \varepsilon_a + \varepsilon_w$).

A basic radiological concept is the activity (of a radioactive source), which is the amount of radionuclides decaying during a given time. In radioactive decay, an unstable isotope attempts to reach stability by emitting radiation in the form of particles and/or electromagnetic waves. After decay, the former isotope is referred to as parent nuclide while the newer is known as daughter nuclide. The number of particles expected to decay ($-\mathrm{d}N$) during a small time ($\mathrm{d}t$) is proportional to the number of particles in the sample (N) and theses quantities are related to each other as:

$$\frac{\mathrm{d}N}{\mathrm{d}t} = -\lambda N \tag{2}$$

where constant λ is the so-called decay constant, whose value is unique for each radioisotope. SI unit for radioactive decay is becquerel (Bq), which is defined as 1 Bq = 1 disintegration per second (dps); yet, curie (Ci) and disintegration per minute (dpm) have also been used.

Knowledge of ^{222}Rn activity concentration profile in phosphogypsum-bearing materials is vital to evaluate resultant exhalation rates. Accordingly, ^{222}Rn transport depends on related mobile activity in the REV, which is properly evaluated and expressed in terms of the partition-corrected porosity ε_c and air-borne activity concentration c_a. For a dry medium without solid sorption, one shows that $\varepsilon_c = \varepsilon$ [88]. Internal sinks of ^{222}Rn activity refers to its decay while internal sources are associated to ^{226}Ra concentration, which can be inferred by assuming that such radioactive impurity is evenly distributed all over the phosphogypsum-bearing material. Corrected emanation rates into the pore system are assessed considering that some ^{222}Rn particles still undergo decay until they finally reach the interstices.

Diffusion-dominant ^{222}Rn transport across porous medium layers is a relatively simple approach valid for low-porosity materials, in which convective transport is neglected while additional simplifying assumptions could include steady-state process and one-dimensional

species transfer. The later implies that porous medium is stratified with regard to a coordinate axis parallel to the main and sole transport direction so that ^{222}Rn concentration becomes uniform at any normal plane. Further steps in the model framework include expansion of the solution domain up to two or three dimensions and time dependence. The later is appropriate for indoor ^{222}Rn accumulation while the former allows one to study edge effects.

Depending on the length scales, one may adopt distinct approaches for the mathematical role of ^{222}Rn exhaling material. A first rationale may assume that the phosphogypsum-bearing material is very slim such as housing panels or boards placed against walls or as part of the building envelope itself [90], [93], [94]. For constant ^{222}Rn diffusivity D_a in open air and disregarding air motion (i.e., neglecting convective mass transfer), ^{222}Rn activity distribution can be governed by the following time-varying diffusive-dominant transport equation [95]:

$$\frac{\partial c_a}{\partial t} = D_a\left(\frac{\partial^2 c_a}{\partial x^2} + \frac{\partial^2 c_a}{\partial y^2} + \frac{\partial^2 c_a}{\partial z^2}\right) - \lambda c_a \tag{3}$$

where x, y and z are Cartesian coordinates, t is time, and sink term ($-\lambda c_a$) is due to ^{222}Rn self-decay. There is no source term (due to emanation) in Eq. (3) as air presumably lacks ^{226}Ra. One may assume that such later radionuclide is uniformly distributed in the phosphogypsum-bearing material thus yielding a fixed and homogeneous ^{222}Rn exhalation rate j_{Rn} into neighboring air. From the mathematical viewpoint, ^{222}Rn exhalation hence becomes a boundary condition rather than a source term in the governing species equation.

Conversely, a distinct approach should be adopted if the solution domain comprises a blunt (i.e., finite thickness) ^{222}Rn exhaling solid as, for instance, a phosphogypsum-bearing building block (brick) in a still-air detection test chamber [94]. In this case, the porous sample partially fills up the solution domain so that ^{222}Rn transport may occur under two distinct "conditions", namely, in open air and within the REV. Corresponding species diffusivities D_a and $\tilde{D}$ can be allegedly constant and conveniently related to each other as:

$$\tilde{D} = \delta D_a \quad \Leftrightarrow \quad \delta = \tilde{D} / D_a \tag{4}$$

where $\tilde{D}$ is the species bulk diffusivity, which should be used whenever species flux j refers to the geometric cross-sectional area A. If Fick's law for ^{222}Rn diffusion is set up in terms of interstitial cross-sectional area, an "interstitial diffusivity"[5] should be used instead [21], [86].

Bearing in mind Eq. (4) and recalling that ^{222}Rn sources (^{226}Ra particles) exist only inside the solid matrix while ^{222}Rn sink (i.e., self-decay) occurs everywhere[6], Eq. (3) is extended to the following diffusive-dominant ^{222}Rn transport equation:

[5] Such transport coefficient has also been referred to as "effective diffusivity" although such term may cause confusion with the usual meaning attributed to "effective" in the porous media literature, which refers the REV averaging procedure previously discussed. "Interstitial diffusivity" should be preferred as it is unambiguous.

[6] Yet, ^{222}Rn self-decay must be properly adjusted with respect to the interstitial volume content.

$$\varepsilon^n \frac{\partial c_a}{\partial t} = \delta^n D_a \left(\frac{\partial^2 c_a}{\partial x^2} + \frac{\partial^2 c_a}{\partial y^2} + \frac{\partial^2 c_a}{\partial z^2} \right) + n\tilde{G} - \varepsilon_c^n \lambda c_a \tag{5}$$

where $\tilde{G}$ is mobile ^{222}Rn activity generation rate per REV unit and the dimensionless parameter n denotes whether ^{222}Rn transport occurs outside (n = 0) or inside (n = 1) the porous matrix [96]. Uniform distribution of ^{226}Ra particles (yielding homogeneous generation rate $\tilde{G}$) and constant partition-corrected porosity ε_c are implicitly assumed in Eq. (5), which can then be regarded an extension to the governing equation proposed in [88].

Radon-222 can be additionally transported by convection, either forced or natural [97]. The former refers to the action of fans, pumps, blowers, or wind while the later is induced by fields (e.g., gravity) acting on density gradients due to thermal and/or solutal variations. Applications point to ^{222}Rn exhaling building envelopes subjected to indoor air currents (thermally induced or not) or to air flow over phosphogypsum-bearing embankments or stacks (piles) [98], [99]. Apart from ^{222}Rn activity governing equation suitably extended to include convective terms, the model framework must equally incorporate bulk fluid continuity and momentum equations to be solved for flow field velocity components. If thermal effects should be accounted for, energy equation is invoked to be usually solved for temperature field. If local thermodynamic equilibrium prevails inside the REV, temperatures are the same for all phases (e.g. solid, air, and water and so that $T_s = T_a = T_w = T$), which is reasonable if internal energy sources are negligible.

Aforesaid governing equations are typically coupled to one another and the corresponding solution domain may encompass both porous medium and open air. With respect to momentum equations, outside the porous material fluid flow can be governed by Navier-Stokes equations, which for Newtonian fluids and incompressible flow (constant density $\rho_a = \rho_\infty$) can be expressed in terms of fluid (air) dynamic viscosity μ_a as:

$$\rho_a \left(\frac{\partial \vec{v}}{\partial t} + \vec{v} \cdot \vec{\nabla} \vec{v} \right) = \mu_a \nabla^2 \vec{v} - \vec{\nabla} p + \rho_a \vec{g} \tag{6}$$

where p is pressure and $\vec{g}$ is gravity acceleration. The so-called seepage (or filtration) velocity $\vec{v}$ has components assessed as $v = \dot{V}/A$, where $\dot{V}$ is the volumetric flow rate through a REV with geometric cross-sectional area A, while components of the so-called interstitial velocity are given as $v_{int} = \dot{V}/A_f$, based on the cross-sectional area $A_f = \varepsilon A$ related to the pore system. Referred to as Dupuit-Forchheimer relation [79], [80], these two velocities are related to each other as:

$$v = \varepsilon v_{int} \qquad \Leftrightarrow \qquad v_{int} = v/\varepsilon \tag{7}$$

Regarding natural convection, Boussinesq approximation can be introduced so that thermo-physical properties become constant except for bulk air density ρ_a in buoyant forces

[97]. Hence, incompressible flow presumably holds while a linear dependence of ρ_a upon local temperature T is supposed solely for the buoyancy term in momentum equations:

$$\rho_a(T) = \rho_\infty\left[1-\beta_T(T-T_\infty)\right] \quad , \quad \beta_T = \frac{1}{\rho_\infty}\left(\frac{\partial \rho_a}{\partial T}\right)_\infty \tag{8}$$

where β_T is the coefficient of thermal volumetric expansion and both density ρ_∞ and temperature T_∞ are reference values such as related to atmospheric air condition sufficiently far from the stack (pile or embankment) or related to indoor air sufficiently far from the building wall. Thinking of thermosolutal natural convection [100], one could claim for radon-induced bulk fluid (air) density variations but corresponding contributions are definitely smaller if compared to entire air mass content so that solutal variations in ρ_a can be safely ignored.

For fluid flow within the porous medium, a classical steady-state approach is Darcy's law relating the fluid velocity $\vec{v}$ and the pressure gradient $\vec{\nabla}p$, namely:

$$\vec{v} = -\frac{1}{\mu_a}\vec{\vec{K}}\cdot\vec{\nabla}p \tag{9}$$

where $\vec{\vec{K}}$ is the permeability tensor [79], [80]. For simplicity, phosphogypsum-bearing materials can be treated as isotropic so that permeability becomes a scalar K and Eq. (9) reduces to:

$$\vec{v} = -\frac{K}{\mu_a}\vec{\nabla}p \quad \Leftrightarrow \quad \vec{\nabla}p = -\frac{\mu_a}{K}\vec{v} \tag{10}$$

It can be further assumed that K is constant throughout. In addition, porosity $\varepsilon = \varepsilon_c$ (dry porous medium without solid sorption) can be supposedly constant all over as well.

Extensions to Darcy's law have been attempted so as to bear some resemblance to Navier-Stokes equations [80]. For the so-called Darcy-Brinkman-Forchheimer approach and in line with [79], [96], [100], [101], [102], [103], one may put forward the following governing equations for bulk fluid mass (continuity), momentum, energy (with local thermal equilibrium but neglecting internal heat sources, viscous dissipation and radiative effects) and species (^{222}Rn activity):

$$\vec{\nabla}\cdot\vec{v} = 0 \tag{11}$$

$$\frac{1}{\varepsilon^n}\frac{\partial\vec{v}}{\partial t} + \frac{\vec{v}\cdot\vec{\nabla}\vec{v}}{(\varepsilon^2)^n} = \Gamma^n\upsilon_a\cdot\nabla^2\vec{v} - \frac{\vec{\nabla}p}{\rho_\infty} - n\left(\frac{\upsilon_a}{K} + \frac{c_f\,|\vec{v}\,|}{\sqrt{K}}\right)\vec{v} + \vec{g}\beta_T(T_\infty - T) \tag{12}$$

$$\left[(1-\varepsilon^n)\rho_s c_s + \varepsilon^n \rho_\infty c_{p,a}\right]\frac{\partial T}{\partial t} + \rho_\infty c_{p,a}\vec{v}\cdot\vec{\nabla}T = \left[(1-\varepsilon^n)k_s + \varepsilon^n k_a\right]\nabla^2 T \tag{13}$$

$$\varepsilon^n \frac{\partial c_a}{\partial t} + \vec{v}\cdot\vec{\nabla}c_a = \delta^n D_a \nabla^2 c_a + n\tilde{G} - \varepsilon^n \lambda\, c_a \tag{14}$$

where $\upsilon_a = \mu_a/\rho_\infty$ is air kinematic viscosity, c_f is a dimensionless form-drag coefficient [80] also referred to as Ergun's coefficient [79], c_s is specific heat of solid matrix, $c_{p,a}$ is constant-pressure specific heat of air while k_s and k_a are thermal conductivities of solid matrix and air, respectively. Depending on porous medium characteristics [79], [80] [102], thermal conductivities of solid (k_s) and air (k_a) can be lumped in a REV-averaged (effective) thermal conductivity obeying a specific expression other than the linear relation in Eq. (13). Analogous to Eq. (4) for ^{222}Rn diffusivity, REV-to-fluid property ratios can also be introduced respectively for kinematic viscosity, thermal conductivity, and heat capacity, as expressed by [101]:

$$\Gamma = \tilde{\upsilon}/\upsilon_a \quad , \quad \Lambda = \tilde{k}/k_a \quad , \quad \sigma = (\tilde{\rho}\tilde{c}_p)/(\rho_\infty c_{p,a}) \tag{15}$$

Modeling ^{222}rn Exhalation from Phosphogypsum-Bearing Materials: Dimensionless Variables

Relying on Buckingham's Π-theorem and similarity rationale [95], transport phenomena models can be expressed by means of dimensionless differential governing equations so that simultaneous influencing parameters can be lumped into fewer controlling parameters. Such practice may help to reduce the number of required experiments, tests, scale-up steps, or optimization procedures. If forced convection prevails regarding open air flow condition, one may choose the free stream velocity u_∞ as a reference value. Applying the previously presented model framework for ^{222}Rn generation and transfer for a two-dimensional domain (without loss of generality), dimensionless variables for time τ, Cartesian coordinates X and Y, velocity components U and V, pressure P, temperature θ, and ^{222}Rn activity concentration C can be defined as:

$$\tau = \frac{t}{\Delta t} \ , \ X = \frac{x}{L} \ , \ Y = \frac{y}{L} \ , \ U = \frac{u}{u_\infty} \ , \ V = \frac{v}{u_\infty} \ , \ P = \frac{p}{\Delta p} \ , \ \theta = \frac{T - T_\infty}{\Delta T} \ ,$$

$$C = \frac{c_a - c_\infty}{\Delta c} \tag{16}$$

where L is a characteristic length while c_∞ is a reference level for ^{222}Rn activity concentration (e.g. in air away from the porous medium) allegedly to fulfill the condition $c_\infty > 0$. Depending on the problem physics, reference scales Δc and ΔT for ^{222}Rn activity concentration and temperature can be suitably defined while proper choices for time and pressure scales are:

$$\Delta t = L/u_\infty \quad \text{and} \quad \Delta p = \rho_\infty u_\infty^2 \tag{17}$$

By introducing Eqs. (16) and (17) into Eqs. (11) to (14) and assuming $\vec{g} = -g\,\hat{j}$, one may write the following set of coupled dimensionless governing equations:

$$\frac{\partial U}{\partial X} + \frac{\partial V}{\partial Y} = 0 \tag{18}$$

$$\frac{1}{\varepsilon^n}\frac{\partial U}{\partial \tau} + \frac{1}{(\varepsilon^2)^n}\left(U\frac{\partial U}{\partial X} + V\frac{\partial U}{\partial Y}\right) = \frac{\Gamma^n}{\mathrm{Re}}\left(\frac{\partial^2 U}{\partial X^2} + \frac{\partial^2 U}{\partial Y^2}\right) - \frac{\partial P}{\partial X} - n\left(\frac{1}{\mathrm{Re\,Da}} + \frac{c_\mathrm{f}\,|\vec{V}|}{\sqrt{\mathrm{Da}}}\right)U \tag{19}$$

$$\frac{1}{\varepsilon^n}\frac{\partial V}{\partial \tau} + \frac{1}{(\varepsilon^2)^n}\left(U\frac{\partial V}{\partial X} + V\frac{\partial V}{\partial Y}\right) = \frac{\Gamma^n}{\mathrm{Re}}\left(\frac{\partial^2 V}{\partial X^2} + \frac{\partial^2 V}{\partial Y^2}\right) - \frac{\partial P}{\partial Y} - n\left(\frac{1}{\mathrm{Re\,Da}} + \frac{c_\mathrm{f}\,|\vec{V}|}{\sqrt{\mathrm{Da}}}\right)V + \frac{\mathrm{Gr}}{\mathrm{Re}^2}\theta \tag{20}$$

$$\sigma^n\frac{\partial \theta}{\partial \tau} + U\frac{\partial \theta}{\partial X} + V\frac{\partial \theta}{\partial Y} = \frac{\Lambda^n}{\mathrm{Re\,Pr}}\left(\frac{\partial^2 \theta}{\partial X^2} + \frac{\partial^2 \theta}{\partial Y^2}\right) \tag{21}$$

$$\varepsilon^n\frac{\partial C}{\partial \tau} + U\frac{\partial C}{\partial X} + V\frac{\partial C}{\partial Y} = \frac{\delta^n}{\mathrm{Re\,Sc}}\left(\frac{\partial^2 C}{\partial X^2} + \frac{\partial^2 C}{\partial Y^2}\right) + \frac{1}{\mathrm{Re\,Sc}}\left[n\mathrm{S} - \varepsilon^n \mathrm{R}(C - C_\infty)\right] \tag{22}$$

where $C_\infty = -c_\infty/\Delta c$ is the C value given by the last of Eqs. (16) for null air-borne ^{222}Rn activity concentration ($c_\mathrm{a} = 0$). Dimensionless parameters regarding convective heat and mass transfer in porous media arise as expected such as Reynolds (Re), Darcy (Da), Grashof (Gr), Prandtl (Pr) and Schmidt (Sc) numbers, expressed in terms of air properties respectively as:

$$\mathrm{Re} = \frac{u_\infty L}{\upsilon_\mathrm{a}} \quad , \quad \mathrm{Da} = \frac{K}{L^2} \quad , \quad \mathrm{Gr} = \frac{g\,\beta_\mathrm{T}\,\Delta T\,L^3}{\upsilon_\mathrm{a}^2} \quad , \quad \mathrm{Pr} = \frac{\upsilon_\mathrm{a}}{\alpha_\mathrm{a}} \quad , \quad \mathrm{Sc} = \frac{\upsilon_\mathrm{a}}{D_\mathrm{a}} \tag{23}$$

where $\alpha_\mathrm{a} = k_\mathrm{a}/(\rho_\infty c_{\mathrm{P,a}})$ is the thermal diffusivity of air.

Besides those parameters, Eq. (22) introduces two unusual dimensionless numbers referred to as decay-to-diffusion (R) and emanation-to-diffusion (S) ratios[7], respectively related to ^{222}Rn decay and emanation processes [93], [94], [98], [99], [104], defined as:

[7] R and S respectively assess the relative importance of ^{222}Rn decay and emanation in relation to its mass diffusion.

$$\mathrm{R} = \frac{\lambda L^2}{D_\mathrm{a}} \quad \text{and} \quad \mathrm{S} = \frac{\widetilde{G} L^2}{D_\mathrm{a} \Delta c} \tag{24}$$

In the model framework for time-dependent pressure-driven ^{222}Rn migration inside soil proposed in [21], two dimensionless groups were introduced in the species (^{222}Rn activity) concentration equation: a convection-to-decay ratio (N) and a mass-transfer Péclet number[8] ($\mathrm{Pe_m}$, measuring the relative importance of convection with respect to diffusion). Recalling the previous definition for the decay-to-diffusion ratio R, Eq. (24), and bearing in mind definitions proposed[9] for N and $\mathrm{Pe_m}$, it is interesting to verify that indeed:

$$\frac{\mathrm{Pe_m}}{\mathrm{N}} = \frac{convection/diffusion}{convection/decay} = \frac{decay}{diffusion} \quad \Rightarrow \quad \frac{\mathrm{Pe_m}}{\mathrm{N}} \cong \mathrm{R} \tag{25}$$

A surrogate dimensionless group M can be additionally introduced[10], namely:

$$\mathrm{M} = \frac{\mathrm{S}}{\mathrm{R}} = \frac{\widetilde{G}}{\lambda \Delta c} \tag{26}$$

which is interpreted as emanation-to-decay ratio [94], [98], [99], [104]. Despite still sensitive to scale Δc for ^{222}Rn activity concentration, M number is independent from both open-air diffusivity D_a and the characteristic length L. In terms of R and M, Eq. (22) can be recast as:

$$\varepsilon^n \frac{\partial C}{\partial \tau} + U \frac{\partial C}{\partial X} + V \frac{\partial C}{\partial Y} = \frac{\delta^n}{\mathrm{Re\,Sc}} \left(\frac{\partial^2 C}{\partial X^2} + \frac{\partial^2 C}{\partial Y^2} \right) + \frac{\mathrm{R}}{\mathrm{Re\,Sc}} \left[n\mathrm{M} - \varepsilon^n (C - C_\infty) \right] \tag{27}$$

In the absence of strong air currents (i.e., negligible forced convection), it might be rather cumbersome to identify a reference velocity u_∞, which can be awkwardly small. Dimensionless variables formerly proposed in Eqs. (16) basically remain the same but suitably "re-scaled" by $u_\infty = \upsilon_\mathrm{a}/L$ wherever required. In Eqs. (19) to (22) or (27), such velocity scale implies that Reynolds number, as defined in line with the first of Eqs. (23), numerically[11] reduces to unity (Re = 1).

PHOSPHOGYPSUM PROPERTIES

Phosphogypsum was characterized from chemical and radiological viewpoint in [105]. One aspect about the later refers to ^{222}Rn exhalation, which is important parameter to assess

[8] There is also a corresponding and similar definition for heat-transfer Péclet number.

[9] It seems the proposed definition for Péclet number should be altered to $\mathrm{Pe_m} = K \Delta P_\mathrm{o} (\varepsilon \mu D)^{-1}$, which apears to be the correct result after casting the proposed governing species transport equation into dimensionless form.

[10] In fact, original definitions for R, S and M included the porosity (either geometric or partition-corrected) [104].

radiation doses onto occupants within dwellings. Indoor ^{222}Rn activity concentration can be experimentally measured using activated charcoal assembled inside relatively simple samplers as the cylindrical one (diameter = 90 mm, height = 45 mm) shown in Figure 20(*a*). Charcoal for measurements must be dried at 75^{o}C for at least 7 days and samplers must be exposed to indoor air for up to 30 days. Retained (adsorbed) ^{222}Rn is counted through gamma spectrometry with NaI detector based on the 609.3 keV peak, which refers to ^{214}Bi radionuclide (a decay product of ^{222}Rn).

Alternatively, solid state nuclear track detectors (SSNTD) have been largely employed due to relatively low cost (related to both detector itself and measurement process), with particular attention to CR-39 polycarbonate (allyl diglycol-cabonate, $C_{12}H_{18}O_7$) detectors presenting higher efficiency. They basically consist of a plastic diffusion chamber that is permeable solely to ^{222}Rn (i.e., decay products of such radionuclide are not able to penetrate through it). As depicted in Figure 20(*b*), SSNTD is placed inside the diffusion chamber in order to register alpha particle emissions occurred during ^{222}Rn decay. A calibration factor correlates the quantity of detected tracks and ^{222}Rn concentration in indoor air.

(*a*) (*b*)

Figure 20. Measurement devices for indoor ^{222}Rn activity concentration: (*a*) activated charcoal collector and (*b*) diffusion chamber with SSNTD.

As far as physical and mechanical properties of interest are concerned, preliminary tests were accomplished in [106] regarding phosphogypsum samples by-produced from 3 distinct phosphate fertilizer industries[12]. Properties were determined considering Brazilian standards for bulk density (NBR 12127), consistency and setting time (NBR 12128, employing a Vicat equipment), modulus of rupture (NBR 12129, utilizing EMIC hydraulic press model PCE 100D - 1 MN load), and free water / crystallization water content (NBR 12130). Brazilian standard NBR 13207 recommends the bulk density of 700 kg·m^{-3} for ordinary gypsum. As preliminary results for phosphogypsum pointed to approximately 570 kg·m^{-3}, results have been improved by properly separating small grains from samples.

The reference value for free water content is 1.3% as specified by NBR 13207. Samples were initially dried at 125ºC for 4 h but results were unsatisfactory for both ordinary gypsum (4.2%) and phosphogypsum (6.2%). After drying samples at the same temperature (125ºC) for a longer period (5 h), improved results were obtained for both phosphogypsum (sample #1 = 0.60%, sample #2 = 0.66%, sample #1 = 1.12%) and gypsum (1.37%). Table 7 shows esults

[11] It is important to stress this is only a numerical implication thanks to the choice of velocity scale.

[12] They are here referred to as numbers, namely, sample #1, sample #2, and sample #3.

for crystallization water content for different drying periods. The phosphogypsum samples were dried up to 7 h in order to fulfill recommended standards (NBR 13207).

Table 7. Crystallization water content (% by mass) for phosphogypsum samples.

Drying period (h)	Sample #1	Sample #2	Sample #3
4	14.43	12.77	n.a. **
5	10.00	9.54	n.a. **
6	9.36	6.77	n.a. **
7	4.91 *	6.22 *	1.34 *
24	5.90 *	6.19 *	1.62 *

* Values fulfilling standards recommended in NBR 13207; ** Not available or not measured.

Table 8 shows the test results for consistency whereas Table 9 shows the results for setting time for both ordinary gypsum and phosphogypsum samples. Regarding the later test, setting starts when the tip remains 1 mm from the base while test ends when tip no longer penetrates into the paste but it just leaves a slender imprint. Compared to ordinary gypsum and phosphogypsum sample #3, either sample #1 or sample #2 required an elevated water consumption, which jeopardized their performance in corresponding MOR tests (as shown ahead). If compared to ordinary gypsum, setting time occurred quite rapidly for phosphogypsum (in general basis), which may affect its handling as it loses its workability faster.

Table 8. Consistency results for ordinary gypsum and phosphogypsum samples.

Amount of gypsum (g)	Cone tip penetration (mm)		Amount of phosphogypsum (g)	Cone tip penetration (mm)		
	Test #1	Test #2		Sample #1	Sample #2	Sample #3
250.00	34	34	187.50	20	21	n.a. **
272.73	36	34	172.50	24	26	n.a. **
300.00	32 *	34	150.00	34	33	n.a. **
319.15	29 *	30 *	157.90	31.5 *	32 *	n.a. **
333.33	24	26	200.00	n.a. **	n.a. **	38
			215.00	n.a. **	n.a. **	29 *
			225.00	n.a. **	n.a. **	25

* Values fulfilling standards recommended in NBR 13207; ** Not available or not measured.

Specimens for MOR tests were prepared in molds with three cubic compartments so that three samples with 50 mm characteristic length were produced simultaneously for each material (ordinary gypsum and phosphogypsum samples). Accordingly, cross-sectional area then results 2500 mm^2 whereas the water/phosphogypsum ratio was the same for consistency

tests. Results for each specimen are presented in Table 10. As already commented, higher water consumption of phosphogypsum in samples #1 and #2 jeopardized their MOR performance. Ordinary gypsum was then added to phosphogypsum as an attempt to improve such property so that new MOR tests for 20% addition (mass basis) resulted in 8.7 MPa and 8.8 MPa for samples #1 and #2, respectively.

Table 9. Setting time results (min:s) for ordinary gypsum and phosphogypsum samples.

Gypsum	Test #1	Test #2	Phosphogypsum	Sample #1	Sample #2
Start	14:30 *	16:00 *	Start	06:00	08:30
End	31:00	31:00	End	09:00	16:26

* Values fulfilling standards recommended in NBR 13207.

Table 10. MOR results for ordinary gypsum and phosphogypsum samples.

Material	Specimen	Load (kN)	MOR (MPa)
Ordinary gypsum	1-G	31.8	12.72 *
	2-G	38.9	15.56 *
	3-G	30.9	12.36 *
Phosphogypsum sample #1	1-A	9.3	3.72
	2-A	5.4	2.16
	3-A	8.8	3.52
Phosphogypsum sample #2	1-B	15.0	6.00
	2-B	10.1	4.04
	3-B	12.3	4.92
Phosphogypsum sample #3	1-C	23.8	9.52 *
	2-C	24.7	9.88 *
	3-C	19.8	7.92 *

* Values fulfilling standards recommended in NBR 13207.

CONCLUSION

Non-conventional building materials have been extensively investigated as an alternative option for cost-effective housing in developing countries. The present chapter addressed and discussed some agroindustrial residues or wastes that are likely to provide a suitable as well as a sustainable solution.

Both waste sisal and banana chemithermomechanical pulps (CTMP) were suitable for cement composite manufacturing via laboratory method similar to counterpart processes broadly used in commercial production. Residual *Eucalyptus grandis* Kraft pulp presented

similar behavior during the fabrication steps of fiber-cement with the advantage of being already available in pulp form and at relatively low costs in comparison to the traditional softwood pulps. The incorporation of these waste fibers at 8% by mass into the matrix based on blast-furnace slag (BFS) resulted in composites with fracture strength approximately 18 MPa slightly lower than the correspondent materials based on ordinary Portland cement (OPC). Both 12% (mass basis) incorporation of sisal and *Eucalyptus grandis* into BFS composites rendered tough composites (approximately 1.2 $kJ \cdot m^{-2}$ of toughness), which is a reasonable performance if compared to previous investigations carried out on sisal chemical pulp as reinforcement for BFS composites.

Microscopy images depicted the importance of proper linkage between composite phases, providing the coexistence of fiber fracture and pullout. Such major outcome could then explain the strength sustained as well as better toughness results achieved by sisal CTMP composites in comparison to corresponding performance of banana CTMP. Physical properties indicated poor packing of high-content fiber composites with the consequent low density and high water absorption values, despite within acceptable standard limits. Both proposed waste fibers utilization and mechanical pulping methods together with low-energy cements as blast-furnace slag are likely to represent an attractive option for asbestos-free fiber-cements in the near future.

Another agroindustrial waste with prospective use as a non-conventional building material is phosphogypsum. Results from its characterization and performance have been quite promising and encouraging. Among possible large-scale exploitation of such by-product one may point to building blocks or housing panels, provided that radiological issues related to radon-222 exhalation and its accumulation in indoor air have been properly overcome. Comprehensive understanding of corresponding transport phenomena is likely to rely on experimental research supported by numerical simulation so as to yield reliable information concerning radiological impact and protection design of prospective safe scenarios.

REFERENCES

[1] Brazilian Government - Ministry of Cities - National Housing Secretary. *Housing Deficit in Brazil*; João Pinheiro Foundation: Belo Horizonte, Brazil, 2006; pp. 20-21.

[2] Agopyan, V.; Cincotto, M. A.; Derolle, A. In: *Proceedings of the 11th CIB Triennial Congress - CIB-89*; CIB: Paris, France, 1989; theme II, vol. I, pp. 353-61.

[3] Agopyan, V.; John, V. M. In: *Fibre reinforced cements and concretes: recent developments*; Swamy, R. N.; Barr, B.; Eds.; Elsevier: London, UK, 1989; pp. 296-305.

[4] Agopyan, V.; Savastano Jr., H.; John, V. M.; Cincotto, M. A. *Cem. Concr. Compos.* 2005, *27*, 527-536.

[5] Agopyan, V. In: *Natural fibre reinforced cement and concrete*; Swamy, R. N.; Ed.; Concrete Technology and Design 5; Blackie: Glasgow, UK, 1988; pp. 208-242.

[6] Coutts, R. S. P. *CSIRO For. Prod. Newsl.* 1986, *2*, 1-4.

[7] Heinricks, H.; Berkenkamp, R.; Lempfer, K.; Ferchland, H. J. In: *Proceedings of the 7th International Inorganic-Bonded Wood and Fiber Composite Materials Conference*; Moslemi, A. A.; Ed.; Siempelkamp Handling Systems Report; University of Idaho: Moscow, 2000; 12 p.

[8] Savastano Jr., H.; Agopyan, V.; Nolasco, A. M.; Pimentel, L. L. *Constr. Build. Mater.* 1999, *13*, 433-438.
[9] Coutts, R. S. P. In: *Proceedings of the 4th International Symposium Fibre Reinforced Cement and Concrete*; Swamy, R. N.; Ed.; E&FN Spon: London, UK, 1992; pp. 31-47.
[10] Gram, H. E. *Durability of natural fibres in concrete*; Swedish Cement and Concrete Research Institute: Stockholm, Sweden, 1983.
[11] Rehsi, S. S. In: Natural Fibre Reinforced Cement and Concrete (Concrete Technology and Design 5); Swamy, R. N.; Ed.; Blackie: Glasgow, UK, 1988; pp. 243-255.
[12] Fordos, Z. In: *Natural Fibre Reinforced Cement and Concrete (Concrete Technology and Design 5)*; Swamy, R. N.; Ed.; Blackie: Glasgow, UK, 1988; pp. 173-207.
[13] Guimarães, S. S. In: *Proceedings of the International Conference Development of Low-Cost and Energy Saving Construction Materials and Applications*; Envo: Rio de Janeiro, Brazil, 1984.
[14] Savastano Jr., H.; Warden, P. G.; Coutts, R. S. P. *Cem. Concr. Compos.* 2005, *27*, 583-592.
[15] Savastano Jr., H.; Turner, A.; Mercer, C.; Soboyejo, W.O. Mechanical behavior of cement-based materials reinforced with sisal fibers. J Mater Sci (2006) 41:6938–6948.
[16] Giannasi, F.; Thebaud-Mony, A. *Int J. Occup. Environ. Health*. 1997, *3*, 150-157.
[17] Brazilian Government - Ministry of Mining and Energy - National Department of Mineral Production (2008). Mineral Summary 2008 - Gypsite (in Portuguese). *http://www.dnpm.gov.br/assets/galeriaDocumento/SumarioMineral2008/gipsita.pdf*.
[18] Rutherford, P. M.; Dudas, M. J.; Samek, R.A. *Sci. Total Environ*. 1994, *149*, 1-38.
[19] UNSCEAR – United Nations Scientific Committee on the Effects of Atomic Radiation. *Sources and Effects of Ionizing Radiation*; United Nations: New York, UN, 2000.
[20] Nero, A. V. In: *Radon and Its Decay Products in Indoor Air*; Nazaroff, W. W.; Nero, A. V.; Eds.; John Wiley & Sons: New York, USA, 1988; pp. 1-53.
[21] Nazaroff, W. W.; Moed, B. A.; Sextro, R. G. In: *Radon and Its Decay Products in Indoor Air*; Nazaroff, W. W.; Nero, A. V.; Eds.; John Wiley & Sons: New York, USA, 1988, pp. 57-112.
[22] Stranden, E. In: *Radon and Its Decay Products in Indoor Air*; Nazaroff, W. W.; Nero, A. V.; Eds.; John Wiley & Sons: New York, USA, 1988, pp. 113-130.
[23] Mazzilli, B.; Palmiro, V.; Saueia, C.; Nisti, M. B. *J. Environ. Radioact.* 2000, *49*,113-122.
[24] U.S. Government (1998). Code of Federal Regulations, Title 40, v. 7, pt. 61.202 (40CFR61.202*). http://www.epa.gov/epahome/topics.html.*
[25] Mazzilli, B.; Saueia, C. *Radiat. Prot. Dosim*. 1999, *86*, 63-67.
[26] ICRP – International Commission on Radiological Protection. *Protection Against Radon-222 at Home and at Work – ICRP Publication 65*; Annals of the ICRP; Pergamon Press: Oxford, UK, 1993; vol. 23/2.
[27] Bentur, A.; Akers, S. A. S. *Int. J. Cem. Compos. Lightweight Concr*. 1989, *11*, 99-109.
[28] Toledo Filho, R. D.; Scrivener, K.; England, G. L.; Ghavami, K. *Cem. Concr. Compos.* 2000, *22*, 127-43.
[29] John, V. M.; Agopyan, V.; Prado, T. A. In: *Proceedings of the 3rd Ibero-American Symposium on Roofing for Housing*; CYTED/USP: São Paulo, Brazil, 1998; pp. 51-59.
[30] Agopyan, V.; John, V. M. *Build. Res. Inf*. 1992, *20*, 233-235.

[31]Savastano Jr., H.; John, V. M.; Caldas, A. In: *Proceedings of the International Conference on Composites in Construction - CCC2001*; Figueiras, J.; Juvandes, L.; Faria, R.; Eds.; Swets & Zeitlinger: Lisse, The Netherlands, 2001; pp. 299-302.

[32]Tonoli, G. H. D.; Santos, S. F.; Joaquim, A. P.; Savastano Jr., H. In: *Proceeding of the 10th International Inorganic-Bonded Fiber Composites Conference*; University of Idaho: São Paulo, Brazil, 2006; 11 p.

[33]Beraldo, A. L. In: *Nonconventional Materials for Rural Construction* (in Portuguese); Toledo Filho, R. D.; Nascimento, J. W. B.; Ghavami, K.; Eds.; Federal University of Paraíba / Brazilian Society of Agricultural Engineering: Campina Grande, Brazil, 1997, pp. 1-48.

[34]Lopes, W. G. R.; Valenciano, M. D. C. M.; Martins, S. C. F.; Beraldo, A. L.; Azzini, A. In: *Proceedings of the International Conference on Sustainable Construction into the Next Millennium: Environmentally Friendly and Innovative Cement Based Materials* (in Portuguese); Barbosa, N. P.; Swamy, R. N.; Lynsdale, C.; Eds.; Federal University of Paraíba / University of Sheffield: João Pessoa, Brazil, 2000, pp. 379-393.

[35]Roma Jr., L. C. *Fibre-cement roofing tiles and cooling system: influence on performance of crossbreed and Holstein veal* (in Portuguese). M. Sc. dissertation; Faculty of Animal Science and Food Engineering, University of São Paulo: Pirassununga, Brazil, 2004.

[36]Savastano Jr., H.; Warden, P. G.; Coutts, R. S. P. *Cem. Concr. Compos.* 2000, *22*, 379-384.

[37]Silva, A. C. *Durability of cellulose fibres reinforced composites* (in Portuguese). M. Sc. dissertation; Polytechnic School, University of São Paulo: São Paulo, Brazil, 2002.

[38]Gram, H. E.; Gut, P. *FCR/MCR Toolkit Element 23 - Quality Control Guidelines*; SKAT, St. Gall, ILO: Geneva, Switzerland, 1991.

[39]Pereira, L. F. L. C.; Cincotto, M. A. *Chlorite determination in concrete of ordinary Portland cement: influence of type of cement* (in Portuguese). Technical Bulletin - BT / PCC / 294; Civil Engineering Department, Polytechnic School, University of São Paulo: São Paulo, Brazil, 2001.

[40]Taylor, H. F. W. *Cement Chemistry*; 2 ed.; Thomas Telford: London, UK, 1997.

[41]Toledo Filho, R. D.; Ghavami, K.; England, G. L.; Scrivener, K. *Cem. Concr. Compos.* 2003, *25*, 185-196.

[42]De Silva, P.; Bucea, L.; Moorehead, D. R.; Sirivivatnanon, V. *Cem. Concr. Compos.* 2006, *28*, 613-620.

[43]Tonoli, G. H. D.; Santos, S. F.; Rabi, J. A.; Santos, W. N.; Akiyoshi, M. M.; Savastano Jr., H. In: *Proceedings of the Brazilian Conference on Non-Conventional Materials and Technologies in Ecological and Sustainable Construction - BRAZIL-NOCMAT*; Ghavami, K.; Toledo Filho, R. D.; Carvalho, R. F.; Eds.; ABMTENC: Salvador, Brazil, 2006.

[44]Alves, S. M.; Pietrobon, C. L. R.; Pietrobon, C. E. In: *Proceedings of the 5th Brazilian Conference on Comfort of Ambient Spaces - ENCAC / 2nd Latin-American Conference on Comfort of Ambient Spaces - ELACAC* (in Portuguese); Pereira, O. R. P.; Eds.; ANTAC: Fortaleza, Brazil, 1999.

[45]Özişik, M. N. *Heat Transfer - A Basic Approach*. McGraw-Hill: New York, USA, 1985.

[46]Brazilian Committee of Civil Construction (CB-02, CE-02:135.07). *Thermal performance in buildings - Calculation methods of thermal transmittance, thermal capacity, thermal delay and solar heat factor of elements and components of buildings* (in Portuguese). ABNT: Rio de Janeiro, Brazil, 1998.

[47]Kawabata, C. Y. *Thermal performance from different types of roof in individual calf housing* (in Portuguese). M. Sc. dissertation; Faculty of Animal Science and Food Engineering, University of São Paulo: Pirassununga, Brazil, 2003.

[48]Devito, R. A. *Physical and mechanical studies of roofing tiles made of blast furnace slag cement reinforced with residual cellulose fibres* (in Portuguese). M. Sc. dissertation; Engineering School of São Carlos, University of São Paulo: São Carlos, Brazil, 2003.

[49]Ferreira, F. L.; Prado, R. T. A. In: *Proceedings of the 20th Conference on Passive and Low Energy Architecture*; Pontifical Catholic University of Chile - PLEA International: Santiago, Chile, 2003.

[50]Oliveira, C.T.A.; John, V.M.; Agopyan, V. Pore water composition of activated granulated blast furnace slag cements pastes. In 2nd International Conference on Alkaline Cements and Concretes, ed. Kiev State Technical University of Construction and Architecture, May 1999, Kiev, 9p. (Accepted paper)

[51]John, V. M. *Slag cement activated with calcium silicates* (in Portuguese). Ph.D. thesis; University of São Paulo: São Paulo, Brazil, 1995.

[52]John, V. M.; Agopyan, V.; Derolle, In: *Proceedings of the 2nd International Symposium on Vegetable Plants and their Fibres as Building Materials*; Sobral, H. S.; Ed.; Chapman and Hall: London, UK, 1990; pp. 87-97.

[53]Higgins, H.G. *Paper physics in Australia*. CSIRO - Division of Forestry and Forest Products: Melbourne, Australia, 1996.

[54]Savastano Jr., H.; Warden, P. G.; Coutts, R. S. P. *Cem. Concr. Compos*. 2003, *25*, 311-319.

[55]Appita - Australian Pulp and Paper Industry Technical Association. *Kappa Number of Pulp*. P201 m-86 (endorsed as part of AS 1301 by the Standards Association of Australia), 1986; 4 p.

[56]Agopyan, V. *Fiber reinforced materials for civil construction in developing countries: use of vegetable fibers* (in Portuguese). University of São Paulo: São Paulo, Brazil, 1991.

[57]Richardson, I. G.; Wilding, C. R.; Dickson, M. J. *Adv. Cem. Res*. 1989, *2*, 147-157.

[58]Douglas, E.; Brandstetr, J. *Cem. Concr. Res*. 1990, *20*, 746-756.

[59]Fernandes, J. D.; Unkalkar, V. G.; Meshramkar, P. M.; Jaspal, N. S.; Didwania, H. P. In: *Nonwood Plant Fiber Pulping*; TAPPI Press: Atlanta, USA, 1981, v. 11, pp. 73-89.

[60]Misra, D. K. In: *Pulp and paper: chemistry and chemical technology*; 3rd. ed.; Casey, J. P.; Ed.; John Wiley & Sons: New York, USA, 1983, v. 1, pp. 504-530.

[61]Coutts, R. S. P.; Kightly, P. *J. Mater. Sci*. 1984, *19*, 3355-3359.

[62]Coutts, R. S. P.; Ridikas, V. *Appita*. 1982, *35*, 395-400.

[63]Soroushian, P.; Marinkute, S.; Won, J. P. *ACI Mater. J*. 1995, *92*, 172-180.

[64]Eusebio, D. A.; Cabangon, R. J.; Warden, P. G.; Coutts, R. S. P. In: *Proceedings of the 4th Pacific Rim Bio-Based Composites Symposium*, Bogor Agricultural University: Bogor, Indonesia, 1998; pp. 428-436.

[65]Soroushian, P.; Shah, Z.; Won, J. P. *ACI Mater. J*. 1995, *92*, 82-92.

[66]Abdelmouleh, M.; Boufi, S.; Salah, A.; Belgacem, M. N.; Gandini, A. *Langmuir*. 2002, *18*, 3203-3208.
[67]Blankenhorn, P. R.; Blankenhorn, B. D.; Silsbee, M. R.; Dicola, M. *Cem. Concr. Res.* 2001, *31*, 1049–1055.
[68]Pehanich, J. L.; Blankenhorn, P. R.; Silsbee, M. R. *Cem. Concr. Res.* 2004, *34*, 59-65.
[69]Xu, Y.; Chung, D. D. L. *Cem. Concr. Res*. 1999, *29*, 451-453.
[70]Britt, K. W.; *Handbook of Pulp and Paper Technology*; 2nd ed.; Van Nostrand Reinhold: New York, USA, 1970.
[71]Clark, J. d'A. *Pulp Technology and Treatment for Paper*; Miller Freeman: San Francisco, USA, 1987.
[72]Coutts, R. S. P. *Composites*. 1984, *15*, 139-143.
[73]Coutts, R. S. P. *J. Mater. Sci. Lett*. 1987, *6*, 140-142.
[74]Mohr, B. J.; Nanko, H.; Kurtis, K. E. *Cem. Concr. Compos*. 2005, *27*, 435-448.
[75]Tonoli, G. H. D.; Joaquim, A. P.; Arsène, M.-A.; Bilba, K.; Savastano Jr., H. *Mat. Manufact. Proc*. 2007, *22*, 1-8.
[76]Bentur, A.; Mindess, S. *Fibre Reinforced Cementitious Composites*; 2nd ed.; Spon Press: London, UK, 2007.
[77]Akkaya, Y.; Picka, J.; Shah, S. P. *J. Mater. Civ. Eng*. 2000, *12*, 272–279.
[78]Chung, D. D. L. 2005. "Dispersion of Short Fibers in Cement". Jounal of Mat. in Civil Engineering 17(4) 379-383.
[79]Kaviany, M. *Principles of Heat Transfer in Porous Media*; Springer: New York, USA, 1995.
[80]Nield, D. A.; Bejan, A. *Convection in Porous Media*; Springer: New York, USA, 1998.
[81]Stranden, E.; Berteig, L. *Health Phys*. 1980, *39*, 275-284.
[82]Stranden, E.; Kolstad, K.; Lind, B. *Radiat. Prot. Dosim*. 1984, *7*, 55-58.
[83]Edwards, J. C.; Bates, R. C. *Health Phys*. 1980, *39*, 263-274.
[84]Loureiro, C. O. *Simulation of the steady-state transport of radon from soil into houses with basements under constant negative pressure*. Ph.D. thesis; Environmental Health Sciences, University of Michigan: Ann Arbor, USA, 1987.
[85]Nazaroff, W. W. *Rev. Geophys*. 1992, *30*, 137-160.
[86]Yu, C.; Loureiro, C.; Cheng, J. J.; Jones, L. G.; Wang, Y. Y.; Chia, Y. P.; Faillace, E. *Data collection handbook to support modeling impacts of radioactive materials in soil*. Environmental Assessment and Information Sciences Division, Argonne National Laboratory: Argonne, USA, 1993.
[87]Riley, W. J.; Robinson, A. L.; Gadgil, A. J.; Nazaroff, W. W. *Atmos. Environ*. 1999, *33*, 2157-2168.
[88]Andersen, C. E. *Radon transport modelling: user's guide to RnMod3d*. Riso-R-1201(EN); Riso National Laboratory: Roskilde, Denmark, 2000.
[89]Nazaroff, W. W., Teichman, K. *Environ. Sci. Technol*. 1990, *24*, 774-782.
[90]Jang, M.; Kang, C. S.; Moon, J. H. *J. Environ. Radioact*. 2005, *80*, 153-160.
[91]Nikezic, D.; Urosevic, V. *Nucl. Instrum. Meth. A*. 1998, *406*, 486-498.
[92]Piliposian, G. T.; Appleby, P. G. *Continuum Mech. Therm*. 2003, *15*, 503-518.
[93]Rabi, J. A.; Silva, N.C. *J. Environ. Radioact*. 2006, *86*, 164-175.
[94]Rabi, J. A.; Silva, N.C. In: *Proceedings of the 11th Brazilian Congress of Thermal Sciences and Engineering – ENCIT 2006*; ABCM – Brazilian Society of Mechanical Sciences and Engineering; Ed.; CD-ROM: Curitiba, Brazil, 2006, CIT06-0428.

[95]Bird, R. B.; Stewart, W. E.; Lightfoot, E. N. *Transport Phenomena*. John Wiley & Sons: New York, USA, 1960.
[96]Mohamad, A.A. *Int. J. Therm. Sci.* 2003, *42*, 385-395.
[97]Kays, W. M.; Crawford, M. E. *Convective Heat and Mass Transfer*. McGraw-Hill: New York, USA, 1993.
[98]Rabi, J. A.; Mohamad, A. A. *J. Porous Media*. 2005, *8*, 175-191.
[99]Rabi, J. A.; Mohamad, A. A. *Appl. Math. Model*. 2006, *30*, 1546-1560.
[100] Bennacer, R.; Beji, H.; Mohamad, A. A. *Int. J. Therm. Sci.* 2003, *42*, 141-151.
[101] Merrikh, A. A.; Mohamad, A. A. *Int. J. Heat Mass Transfer*. 2002, *45*, 4305-4313.
[102] Ingham, D. B. In: *Current Issues on Heat and Mass Transfer in Porous Media*; Ingham, D. B.; Ed.; NATO Advanced Study Institute on Porous Media; Ovidius University Press: Constanța, Romania, 2003, pp. 1-10.
[103] Askri, F.; Ben Salah, M.; Jemni, A.; Ben Nasrallah, S. In: *Applications of Porous Media*; Reis, A. H.; Miguel, A. F.; Eds.; ICAMP 2004; CGE: Évora, Portugal, 2004, pp. 315-318.
[104] Rabi, J. A.; Mohamad, A. A. In: *Applications of Porous Media*; Reis, A. H.; Miguel, A. F.; Eds.; ICAMP 2004; CGE: Évora, Portugal, 2004, pp. 471-478.
[105] Silva, N. C. *Natural radionuclides and toxic elements within phosphogypsum stacks in Brazil: characterization and lixiviation* (in Portuguese). Ph.D. thesis; University of São Paulo: Piracicaba, Brazil, 2001.
[106] Rabi, J. A.; Silva, N. C.; Soares, S. M.; Prado, A. S.; Santos, A. R. In*: Proceedings of the Inter-American Conference on Non-Conventional Materials and Technologies in Ecological and Sustainable Construction* - IAC-NOCMAT; Ghavami, K.; Savastano Jr., H.; Joaquim, A. P.; Eds.; ABMTENC: Rio de Janeiro, Brazil, 2005.